AD-A172 770 THE RAY-INTEGRATION TECHNIQUE IN SPHERICAL GEOMETRY(U) 1/2
AIR FORCE INST OF TECH WRIGHT-PATTERSON AFB OH SCHOOL
OF ENGINEERING S E DURHAM MAR 86 AFIT/GNE/ENP/86M-3

UNCLASSIFIED F/G 20/9 NL

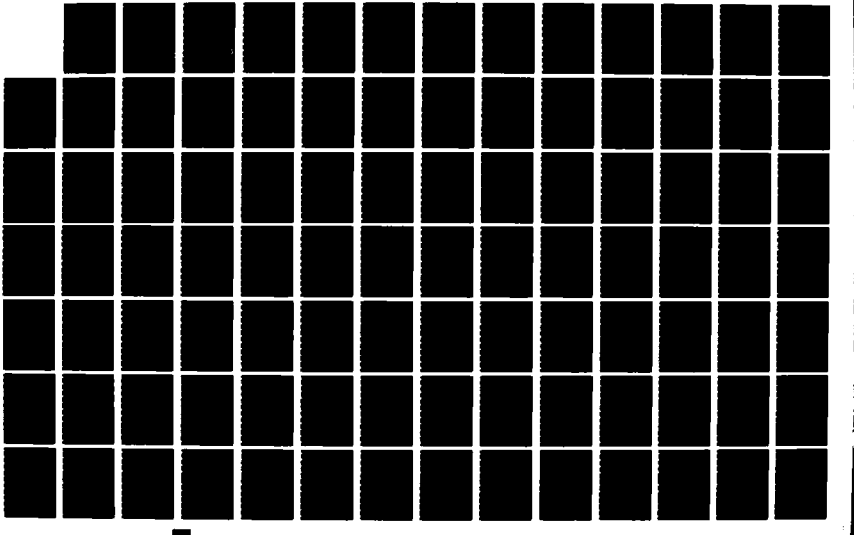

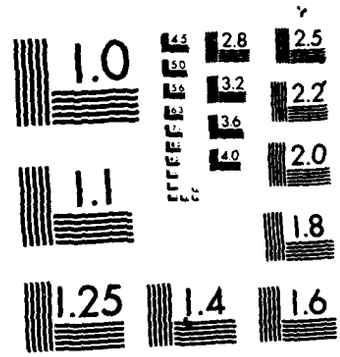

THE RAY-INTEGRATION TECHNIQUE IN SPHERICAL GEOMETRY

THESIS

Susan E. Durham
First Lieutenant, USAF

AFIT/GNE/ENP/86M-3

DEPARTMENT OF THE AIR FORCE
AIR UNIVERSITY
AIR FORCE INSTITUTE OF TECHNOLOGY

Wright-Patterson Air Force Base, Ohio

AFIT/GNE/ENP/86M-3

THE RAY-INTEGRATION TECHNIQUE IN SPHERICAL GEOMETRY

THESIS

Susan E. Durham
First Lieutenant, USAF

AFIT/GNE/ENP/86M-3

Approved for public release; distribution unlimited

AFIT/GNE/ENP/86M-3

THE RAY-INTEGRATION TECHNIQUE IN SPHERICAL GEOMETRY

THESIS

Presented to the Faculty of the School of Engineering
of the Air Force Institute of Technology
Air University
In Partial Fulfillment of the
Requirements for the Degree of
Master of Science in Nuclear Science

Susan E. Durham, B.S.
First Lieutenant, USAF

March 1986

Acknowledgements

Every scientific composition is a collaborated effort. The research, responses and reporting are based, in some way, on the assistance and inspiration of others. I would like to acknowledge some of my most valuable fellow "collaborators". Special thanks to Dr. George Nickel, my thesis advisor, for giving me the opportunity to pursue a subject of personal interest. Especially, I would like to thank Dr. Nickel for his time in making graphs and helping me construct vital portions of the computer code. His concerned tutoring and valuable advice is the cornerstone to the successful completion of this research.

I also would like to express my sincere appreciation to Dr. Charles Bridgman who directed my thesis work at AFIT and allowed me much freedom of approach while simultaneously providing a sense of direction and perspective. Especially, thanks to Dr. Bridgman for his constant insistence to see "the big picture; the rest are details".

Thanks, also, to a good friend, Corbett Elliott, for working magic with my often temperamental computer system.

Most importantly, I am extremely grateful to my husband, Bob Bigrigg, without whose unselfish patience and moral support, my work at AFIT would have been not only unbearable, but meaningless.

Susan E. Durham

Table of Contents

List of Figures

List of Tables

Abstract

A method of solution for the equation of radiative transfe for a spherical, grey atmosphere, steady state plasma in radiative equilibrium is developed. The method is called the ray-integration technique and derives from the same method of solution done in cylindrical geometry by George Nickel of Los Alamos National Laboratory. The total and net radiation flux, source function, opacity and moments of intensity are calculated as a function of radius. The solution to the zero'th and first moment equations are also provided.

The conditions of the grey atmosphere problem and the general nature of radiation transport in spherical geometry are developed and the ray integration technique, as applied to the problem, is presented.

Numerical results are calculated for a variety of radial mesh and opacities. These results are provided in graphic form and compared against theoretically predicted behavior.

The ray-integration technique developed in this thesis produces numerical results which are in reasonable agreement with theoretical predicted results.

THE RAY-INTEGRATION TECHNIQUE IN SPHERICAL GEOMETRY

I. Introduction

Background

Motivation. In any study of radiative energy transport, the formulation and solution of a fundamental conservation equation is of paramount importance. This equation is known as the equation of radiative transfer, or, more commonly, the transfer equation. The transfer equation predicts the character of the radiation field of a plasma by solving for the intensity at a point within the field as function of time and position. This thesis prescribes a method of solution to the transfer equation in a one-dimensional, steady-state, frequency independent medium in one-dimensional spherical geometry.

The method used is called the ray-integration technique and is based on work done by George Nickel of Los Alamos National Laboratory.

TRAILMASTER Project. The ray-integration technique is derived from work done by Nickel in support of the U. S. Air Force's TRAILMASTER project. The goal of this project is to create a high energy source of soft X-rays from the rapid collapse of a cylindrical foil. In support of this goal, Dr. Nickel created a program called LMILNE which executed the ray-integration technique in cylindrical geometry. The program he

created incorporated some techniques which could be expanded, with modification, to different geometries. It was determined that so modifying the technique into spherical geometry would prove useful.

General Applicability. A solution for the transfer equation is frequently needed in many branches of physics. The preponderance of dense spherical plasmas with radiation fields modeled in research provides the motivation to find methods of solution which are both efficient and accurate. The ray-integration method has proved to be both.

Analysis of Stellar Atmospheres. Applied to spherical geometry, the ray-integration method of solving the equation of radiative transfer could be very useful, especially to the astrophysics community as a "first order estimate" device for modeling extended stellar atmospheres. The assumptions made about the nature of the plasma system solved for in this investigation is completely analagous to the radiative equilibrium, grey atomosphere model often used in text books to illustrate the basic nature of radiation transport. The research for this thesis depended extensively on this analogy. Although normally referring to a stellar body, the terms atmosphere and interior are used throughout this paper to refer to the regions of energy transport and source region respectively. This in no way alters the applicability of the assumptions and solutions to spherical plasmas in general.

Objectives and Scope

The goal of this research has been to produce a physically realistic solution to the transfer equation which:

-- produces numerically accurate results from which the character of a plasma can be approximated

-- can be used to engender an intuitive understanding of the physical nature of stellar atmospheres.

A second objective of this research is to verify the ray-integration technique as plausible by:

-- implementing a computer program which utilizes this technique

-- producing graphs of the results using various combinations of radii, opacity, power and iteration techniques

-- comparing the results of this program against theoretically predicted results.

Assumptions

To effectively develop a method of solution for the behavior of a system, its physical character must be established. That is, assumptions about the size, shape, and material properties of the system, in this case, the plasma, must be known beforehand. This does limit the applicability of a technique to a specific physical model, but often provides sufficient insight to generalize the method to other systems.

The particular assumptions made are that the ray-integration technique, as developed in this thesis, is applicable specifically to a system that is

-- spherical

-- frequency independent (called the grey atmosphere problem)

--in radiative equilibrium

-- time invariant, i.e. steady state.

Method of Solution

The ray-integration technique is implemented using a computer program written in the FORTRAN language. The program was executed on both a CRAY located at Los Alamos National Laboratory and, with minor changes, on the author's APPLE II+ compatible computer. The graphs shown in this report were done exclusively on the CRAY.

The inputs to the program were values for the opacity and source function of the radiation, as well as the number of radii and radii spacing which consequently made up the radii mesh.

The output of the program is the net radiation flux, the total radiation flux, and the ratio of moments of intensity known as the Eddington Factors. Additional output consists of solutions to the moments of the transfer equation. All input and output are in MKS units.

Plan of Presentation

This report is presented in the following manner. The first chapter is a review of the basic theories of radiation transport and of the specific nature of the grey atmosphere problem in radiative equilibrium. Chapter II presents an

overview and develops the ray-integration technique. The next chapter provides a development of the numerical methods. This is followed by an outline of the program developed to implement the ray-integration technique. Next presented is a summary of some results generated by the computer code, along with a discussion of these results. Finally, conclusions and recommendations for further study are put forth in the last chapter.

II. Theory

To understand the technique for solving the equation of radiative transfer, it is first necessary to review some of the basic physical theories of the transfer of energy and develop the transfer equation for analysis. This will be done in this section beginning with the characteristics of the radiation field and progressing through a general description of the grey atmosphere. The development of the following concepts is fairly standard and can be found in many textbooks such as references 2, 3, 6, 7, and 9.

Description of the Radiation Field

The region within and surrounding the body of a star or spherical plasma mass is a radiation field which contains photons of various frequencies traveling in all directions. The interaction of the photons with the mass of the body and with each other results in energy transfer. A description of the intensity variations, then, describe the nature of the radiation field from which other material properties of the mass may be derived.

Specific Intensity. The radiation field produced by the emission and absorption of photons brings about a transport of radiant energy, dE, in a specified energy interval $(\nu, \nu + d\nu)$. Picture this energy transfer as a beam of radiation flowing from a surface element area dA, into a solid angle $d\Omega$, in a direction Ω that makes an angle (φ) with the normal to the

surface, $\hat{n}$, (see Figure 1).

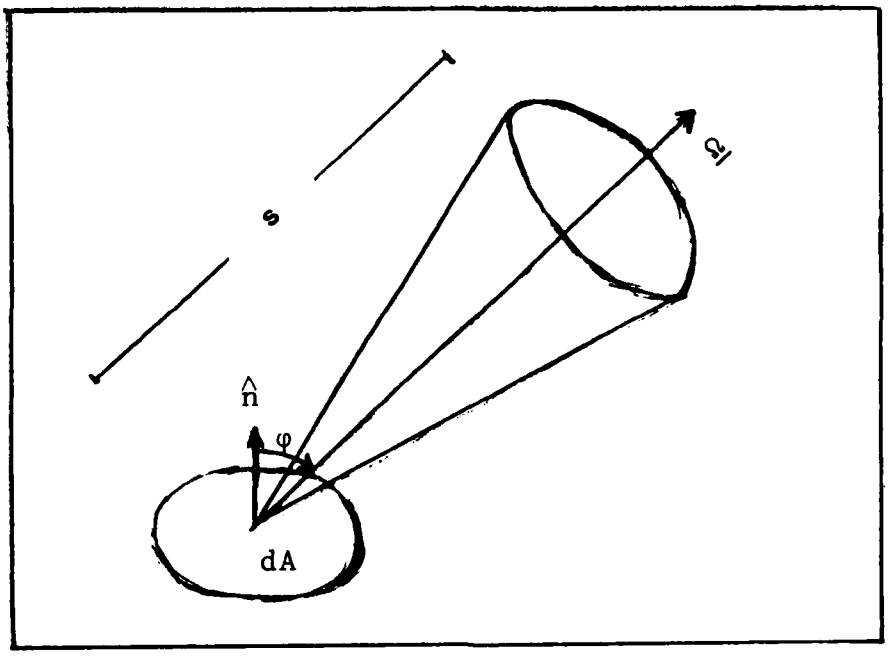

Figure 1

A beam of radiation, originating from surface element dA, into a solid angle dΩ, travelling in direction $\underline{\Omega}$ of length s.

The transfer of energy along a distance r and through time interval dt is expressed by the equation

$$dE(\underline{n},\underline{s},\nu,t) = I(\underline{n},\underline{s},\nu,t)\, d\Omega\, dt\, d\nu\, \cos(\varphi)\, ds \qquad (1)$$

where $I(\underline{n},\underline{s},\nu,t)$ is defined as the specific intensity (or, more simply, intensity). Suppressing the time and spatial dependence, intensity = I_ν. The units of intensity are watts m^{-2} sr^{-1} hz^{-1}. It is clear that, by knowing the specific intensity at points progressing through a region, the energy present, and many quantities derivable from the energy, can

be known.

Moments of Intensity

The Mean Intensity. In addition to intensity, there are other quantities used frequently to describe the behavior of the radiation field. These are the angular averages, or the angular moments, of intensity. There are three moments which are used in spherical geometry. The first is called the zero'th order moment or the mean intensity, J, and is simply the average of the intensity over all angles (thus, it is often also called the "all-angle intensity"). The mean intensity is, therefore, given by

$$J_\nu = \frac{1}{4\pi} \int_\Omega I_\nu \, d\Omega \tag{2}$$

The units of J_ν are the same as the units for I_ν.

It is common practice to transform the integral over solid angles to an integral over the quantity $\mu = \cos(\varphi)$. This is done by substituting the differential $d\Omega$ by $\sin(\varphi)\, d\vartheta\, d\varphi = -\, d\vartheta\, d\mu$. If, as is usually the case, there is symmetry about the azimuthal direction, then the integral becomes

$$J_\nu = \frac{1}{2} \int_{-1}^{1} I_\nu(\mu)\, d\mu \tag{3}$$

Expressing the angular moments in terms of integrals in μ is known as Eddington notation.

The Flux. The first order moment of intensity is known as the flux, ξ_ν. Physically, this flux represents a vector quantity such that $(\xi_\nu \cdot dA)$ gives the radiation energy flow across a surface area dA per unit time, per unit frequency interval. Analytically, this is given by

$$\xi_\nu = \int_\Omega I_\nu(\Omega) \cos(\varphi) \, d\Omega \tag{4}$$

In Eddington notation, this integral becomes

$$\xi_\nu = 2\pi \int_{-1}^{1} I_\nu (\mu) \, \mu \, d\mu \tag{5}$$

The units of total radiation flux are watts m^{-2} hz^{-1}. Additionally, a quantity called the Eddington flux is defined as

$$H_\nu = \frac{1}{4\pi} \xi_\nu = \frac{1}{2} \int_{-1}^{1} I_\nu(\mu) \, \mu \, d\mu \tag{6}$$

It can be seen that the Eddington Flux is an average flux per steradian. Its units are watts $m^{-2} str^{-1} hz^{-1}$.

One other commonly seen version of the radiation flux is called the astrophysical or total flux, F. This is simply the flux emitted over all directions and is

$$F_\nu(r) = 4\pi r^2 \, H_\nu \tag{7}$$

where r is the distance from the center of the sphere to the location at which the flux is being evaluated.

The Second Moment. The second moment of intensity, K, is related to the radiation pressure (3:68). This quantity is simply constructed by multiplying the intensity by $\cos^2(\varphi)$ and integrating over all solid angles. Using Eddington notation,

$$K_\nu = \frac{1}{2} \int_{-1}^{1} I_\nu (\mu)\ \mu^2\ d\mu \qquad (8)$$

The units for K are the same as for I_ν, J_ν, and H_ν.

Summary. The traditional radiation quantities I, J, H, and K, described in the last sections are generally sufficient to develop an approximate analysis of the radiation field. For emphasis and easy referral, they are summarized in Table 1. The equations are given in Eddington notation because this the form will be used throughout the remainder of this report.

Table I

Summary of Intensity and Moments of Intensity

Nomenclature	Symbol	Equation
Intensity	I_ν	$dE = I_\nu\ d\Omega\ dt\ d\nu\ \cos(\varphi)\ ds$
Mean Intensity (Zero Moment)	J_ν	$J_\nu = \frac{1}{2} \int_{-1}^{1} I_\nu(\mu)\ d\mu$
Eddington Flux (First Moment)	H_ν	$H_\nu = \frac{1}{2} \int_{-1}^{1} I_\nu(\mu)\ \mu\ d\mu$
Second Order Moment	K_ν	$K_\nu = \frac{1}{2} \int_{-1}^{1} I_\nu(\mu)\ \mu^2\ d\mu$

The Interaction of Radiation with Matter

Having thus defined the quantities which approximate the radiation field, we now consider the processes which produce and modify them.

Interaction Processes. Photons are catagorized into specific energy groups of given frequency intervals. The photons, as they pass through the matter in the radiation field, constantly interact with that matter and with each other. They may be scattered out of an energy interval or absorbed by atoms, ions or molecules. They may be emitted into energy groups by spontaneous decay, or simply scattered into an energy group as a result of being scattered out of another. The result of these interactions is to modify the intensity of the radiation field. Detailed descriptions of these processes are not necessary for the comprehensive development of this thesis. It is sufficient to separate these interaction processes into two groups, removal mechanisms and addition mechanisms, and consider only the microscopic results of the processes in terms of opacity and emissivity.

Opacity. The probability that a photon will be either scattered or absorbed in a prescribed path length is given by the extinction coefficient, or opacity, χ_ν. The opacity, in general, is defined in a similar manner as the intensity. That is, the amount of material removed can be represented by an energy flow, such that a volume of material of cross section dA, and length da, removes from a beam with specific intensity I_ν, incident normal to dA and propagating into a solid angle $d\Omega$, an

amount of energy

$$\delta E(\underline{n},\underline{s},\nu,t) + \chi(\underline{n},\underline{s},\nu,t)\ I(\underline{n},\underline{s},\nu,t)\ dA\ da\ d\Omega\ dt \qquad (9)$$

within a frequency interval $d\nu$, in a time dt (5:23).

There are different opacities for scattering and for absorption, and even different opacities for the categories of scattering (elastic, coherent, etc.) and for the types of absorption that occur (photonization, free-free absorption, etc.) However, since these processes are statistically independent, the opacities add linearly such that

$$\chi_\nu{}^T = \chi_\nu{}^s + \chi_\nu{}^a \qquad (10)$$

where $\chi_\nu{}^s$ is the scattering opacity, $\chi_\nu{}^a$ is the absorption opacity and $\chi_\nu{}^T$ is the total materials opacity. For convenience, in this thesis, no distinction will be made between the particular type of removal mechanism and the term opacity will be used to refer to the total material opacity. Since opacity is the probability that a photon will interact over a given distance, the inverse of the opacity is simply the mean distance that a photon will go before an interaction occurs, i.e., the inverse of the opacity is the mean free path. The units of opacity are length^{-1}; or m^{-1}.

Emissivity. The population of photons in a frequency interval may be altered not only by removal from the interval, but also by addition to the interval from other frequency

groups. This may be done either by the photons being scattered into the group as they were scattered out of others, or they may be created by some emission process.

Following the process used to define the extinction coefficient, we define the emission coefficient, or emissivity, η_ν, such that the amount of energy released from an element of material of cross section dA and length da into a solid angle $d\Omega$, within a frequency band $d\nu$, in direction $\underline{\Omega}$ in a time interval dt, as

$$\partial E(\underline{n},\underline{s},\nu,t) = \eta_\nu(\underline{n},\underline{s},\nu,t)\ dA\ da\ d\Omega\ d\nu\ dt \tag{11}$$

The units of emissivity are watts $m^{-2}sr^{-1}hz^{-1}$ (7:25). Again, the above derived quantity is the total emissivity and is a linear sum of emissivities of the separate emission processes.

Optical Depth and the Source Function

Having defined the concept of opacity and emissivity, two very important concepts are presented which derive from the above. These are the optical depth and the source function.

The Optical Depth. Given the opacity along a path length ds, the differential optical thickness is defined such that

$$d\tau_\nu = \chi_\nu\, ds \tag{12}$$

Integrating over a distance along the line of sight yields

$$\tau_\nu(s) = \int_{s_1}^{s_2} \chi_\nu(s')\, ds' \tag{13}$$

where τ_ν is now the optical depth. Since ds is in units of distance and χ_ν is in units of inverse distance, τ_ν is dimensionless. The limits s1 and s2 are defined such that the integral is always positive, that is the optical depth increases as r -> 0 and is 0 at the surface of the sphere. The optical depth is the number of mean free paths along the line of sight. A region is said to be "optically thick" if $\tau_\nu >> 1$, and "optically thin" if $\tau_\nu << 1$.

The Source Function. As stated in section B, the radiation field is continually being perturbed by the removal and addition of photons. The ratio of the amount added to the amount removed is simply the ratio of the emissivity to the opacity and is called the source function, S. The source function is, then, given by

$$S_\nu = \frac{\eta_\nu}{\chi_\nu} \qquad (14)$$

where χ_ν is the total opacity and η_ν is the total emissivity. Although simply defined, the source function can actually be quite involved to calculate, depending on the number of processes occurring which produce the opacity and emissivity of the material. An excellent treatment of some of the more common variations of the source function can be found in Reference 7, Chapter 2 and Reference 2.

The Transfer Equation

The material properties, opacity and emissivity, discussed

in Section C, modify the intensity of a stellar atmosphere. The change produced can be expressed in words as

[change in I per path length ds] = [source - sinks] (15)

where the term "sources" means change in intensity per path length ds due to the emission processes occurring, and "sinks" refers to the changes occurring which are due to absorption. Thus, the above can be rewritten in terms of opacity and emissivity as

$$\frac{dI}{ds} = \eta_\nu - \chi_\nu I_\nu \tag{16}$$

where χ_ν is the total materials opacity and η_ν is the total materials emissivity. Expressing the left hand side explicitly in terms of position and time yields

$$\frac{dI_\nu}{ds} = \frac{1}{c}\frac{\partial I_\nu}{\partial t} + \underline{\Omega} \cdot \nabla I_\nu \tag{17}$$

Coupling equations (16) and (17),

$$\frac{1}{c}\frac{\partial I_\nu}{\partial t} + \underline{\Omega} \cdot \nabla I_\nu = \eta_\nu - \chi_\nu I_\nu \tag{18}$$

which is the transfer equation in differential form. Using (14) and assuming a steady-state radiation field,

$$\underline{\Omega} \cdot \nabla I_\nu = \chi_\nu (S_\nu - I_\nu) \tag{19}$$

For a one-dimensional, spherically symmetric radiation field,

$$\cos(\varphi)\,\frac{\partial I}{\partial r} - \frac{\sin(\varphi)}{r}\,\frac{\partial I}{\partial \varphi} = \chi_\nu (S_\nu - I_\nu) \tag{20}$$

In terms of Eddington notation, this is

$$\mu\,\frac{\partial I}{\partial r} + \frac{(1-\mu^2)}{r}\,\frac{\partial I}{\partial \mu} = \chi_\nu (S_\nu - I_\nu) \tag{21}$$

Yet another form of the equation (19) is produced using the definition of the source function and the relationship $d\tau_\nu = \chi_\nu dS$, such that

$$\frac{dI_\nu}{d\tau} = S_\nu - I_\nu \tag{22}$$

Multiplying both sides of the above by , and integrating over $d\tau$, from $\tau_\nu' = 0$ to $\tau_\nu' = \tau_\nu$. The result is

$$I_\nu(\tau_\nu) = I_\nu(o)\, e^{-\tau_\nu} + \int^{\tau_\nu} S_\nu\, e^{(\tau_\nu' - \tau_\nu)}\, d\tau_\nu' \tag{23}$$

A number of variations of the transfer equation have been presented in this section. To review, and for the convenience of the reader, the following table lists the version of the transfer equation and its solution which will appear explicitly in a later section.

Table II

The Transfer Equation and its Solution for a One-Dimensional, Spherically-Symmetric Radiation Field

Name	Equation
Transfer eq. in spherical coordinates	$\mu \frac{\partial I_\nu}{\partial r} + \frac{1-\mu^2}{r} \frac{\partial I_\nu}{\partial \mu} = \chi_\nu (S_\nu - I_\nu)$
Solution to the transfer eq.	$I_\nu(\tau_\nu) = I_\nu(o)e^{-\tau_\nu} + \int_o^{\tau_\nu} S_\nu e^{(\tau_\nu' - \tau_\nu)} \, \tau_\nu'$

The Moments Equations

As the transfer equation represents the change in intensity, so the moments equations represent changes in the moments of intensity. These equations will now be presented.

The Zero'th Moment Equation. The zero'th moment equation is formed from equation (21). Integrating this equation over all solid angles or, in Eddington notation integrating over μ from -1 to 1, yields

$$\frac{1}{2}\int_{-1}^{1} \mu \frac{\partial I_\nu}{\partial r} \, d\mu + \frac{1}{2}\int_{-1}^{1} \frac{(1-\mu^2)}{r} \frac{\partial I_\nu}{\partial \mu} \, d\mu = \frac{1}{2}\int_{-1}^{1} \chi_\nu (S_\nu - I_\nu) \, d\mu \quad (24)$$

Using the relation

$$\frac{1}{2}\int_{-1}^{1} \mu^n \frac{\partial I_\nu}{\partial \mu} \, d\mu = \frac{1}{2}\int_{-1}^{1} \frac{\partial(\mu^n I_\nu)}{\partial \mu} \, d\mu - \frac{1}{2}\int_{-1}^{1} n\mu^{n+1} I_\nu \, d\mu \quad (25)$$

Equation (24) becomes

$$\frac{\partial}{\partial r}\left[\frac{1}{2}\int_{-1}^{1}\mu\ I_\nu\ d\mu\right] + \frac{1}{r}\left[-\frac{1}{2}\int_{-1}^{1}\mu\ I_\nu\ d\mu\right] = \frac{\chi_\nu^{s}}{2}\int_{-1}^{1}d\mu + \frac{\chi_\nu}{2}\left[\int_{-1}^{1} I_\nu\ d\mu\right] \quad (26)$$

Substituting in for the boxed quantities, those moments they equate to (see Table I, page 10) the zero'th moment equation is revealed to be

$$\frac{\partial H_\nu}{\partial r} + \frac{2}{r} H_\nu = \frac{1}{r^2}\frac{\partial(r^2 H)}{\partial r} = \chi_\nu\ (S_\nu - J_\nu) \quad (27)$$

The First Moment Equation. Proceeding in the same manner as above, equation (21) is this time multiplied through by μ and integrated over all μ. Again using relation (25) produces

$$\frac{\partial}{\partial r}\left[\frac{1}{2}\int_{-1}^{1}\mu^2 I_\nu\ d\mu\right] + \frac{1}{r}\left[-\frac{1}{2}\int_{-1}^{1} I_\nu\ d\mu + \frac{1}{2}\int_{-1}^{1} 3\mu^2 I_\nu\ d\mu\right] = -\chi_\nu\frac{1}{2}\left[\int_{-1}^{1} I_\nu\ d\mu\right] \quad (28)$$

Again, substituting the appropriate moments from Table I yields the first moment equation.

$$\frac{\partial K}{\partial r} + \frac{3K - J}{r} = -\chi_\nu H_\nu \quad (29)$$

Summary. For emphasis, the following table lists the significant equations of this section.

Table III

The Moment Equations

Name	Equation	
Zero'th Moment Eq.	$\frac{1}{r^2}\frac{\partial(r^2 H_\nu)}{\partial r} = \chi_\nu (S_\nu - J_\nu)$	(27)
First Moment Eq.	$\frac{\partial K_\nu}{\partial r} + \frac{3K_\nu - J_\nu}{r} = -\chi_\nu H_\nu$	(29)

Assumptions and Approximations

Vital to any scientific work are the assumptions and approximations that are made. Already certain approximations have been presented in this thesis. In Section C, the approximate regions traditionally considered optically thick or thin were outlined. In Section B, causally different inter-atomic processes were grouped under the same headings as either removal or addition mechanisms. The transfer equation in Section D was specialized, based on a steady state approximation. All these are valid in general and essential to the development of this thesis. In this section, the last approximations and assumptions necessary to be stated are presented.

The Eddington Approximation. The material properties, opacity and emissivity modify the energy flow and, thus, the intensity and its moments. In particular, within certain limits of optical thickness, the moments take on approximate values. This section discusses one very frequently used ap-

proximation, the Eddington approximation, and variations of it.

The Eddington Factor.

The Diffusion Limit. The Eddington approximation is manifested in the variable Eddington factor, f_k, which is defined as the ratio of the second moment of intensity to the zero'th, or, more simply, $f_k = K/J$. The approximation is that, at great optical depths, the radiation field is nearly isotropic. The area where this is true is called the diffusion limit. In this limit, the intensity is subsequently independent of angle and can be removed from the moments integrals of Table II, page 17. Doing so reduces those equations to

$$J_\nu = I_\nu \frac{1}{2} \int_{-1}^{1} d\mu = I_\nu \tag{30}$$

and

$$K_\nu = I_\nu \frac{1}{2} \int_{-1}^{1} \mu^2 \, d\mu = \frac{I_\nu}{3} \tag{31}$$

Thus, in the diffusion limit, $f_k = 1/3$. This is physically valid and can be derived independently as part of the diffusion approximation (7:51).

The Streaming Limit. While the Eddington approximation certainly holds true in the optically thick regions of the plasma, what then can be said about its accuracy in the optically thin, less dense, outer regions? In this case, the Eddington Approximation must be augmented.

Consider that, in the outer region, the photons are no

longer colliding as frequently, since their population is, by definition, sparse. Thus, the mean free path is comparatively long and the photons can be thought of as essentially traveling in uninterrupted paths or, streaming. In this streaming limit, all photons are going in the same "direction": out. Therefore, all angular moments must sum to the same value and any ratio, thereof, must be one, thus the Eddington factor, f_k, is one in the streaming limit. It is, therefore, more accurate to talk about not an Eddington factor, but a variable Eddington factor: one which varies from 1/3 at deep optical depths within the system to 1 at the outer boundry of the system.

The "Second" Eddington Factor. Although most literature refers only to the ratio f_k as the Eddington factor, there is also another comparative ratio which is frequently used. This is the ratio of the Eddington flux to the mean intensity, or H/J. This "second" Eddington factor will be referred to in this thesis as f_H. For convenience, both ratios will be termed the Eddington factors and will be distinguished by their subscripts. As with the first Eddington factor, the ratio H/J also has limiting values.

The Flux as r -> 0. In the central regions of the sphere, it is clear to see that f_H must be zero. This is due to the fact that as r -> 0, the radiation field is isotropic and, thus, the total radiation flux must be zero, since there is no net energy flow. Analytically, this can be seen by returning to Table II and noting that for an isotropic

field I is, by definition, independent of and can be removed from the integral. What remains then is

$$H_\nu = I_\nu \frac{1}{2}\int_{-1}^{1} \mu \, d\mu = 0 \tag{32}$$

Thus, if H -> 0, as r -> 0, so to does f_H.

The Streaming Limit. In the streaming limit f_H -> 1. This is so for the same reasons given previously for the streaming limit approximation of f_k.

Radiative Equilibrium. A stellar atmosphere by definition is that portion of the star that transmits the radiation which is created deep within the interior. In the atmosphere region, these energy transfer processes take on two forms in general: radiative and hydrodynamic. For the purposes of this thesis, it is assumed that all transfer processes are radiative. In other words, it is assumed that the plasma system is in radiative equilibrium; that is, all energy is transferred through radiative processes, thus all energy absorbed in a volume element must equal that radiated in that element. If over all frequency intervals, the energy removed from the beam is

$$\int_0^\infty d\nu \oint d\Omega \, \chi_\nu \, I_\nu = 4\pi \int_0^\infty \chi_\nu \, J_\nu \, d\nu \tag{33}$$

And the energy emitted is

$$\int_0^\infty d\nu \oint d\Omega \, \eta_\nu = 4\pi \int_0^\infty \chi_\nu \, S_\nu \, d\nu \tag{34}$$

This results in the relation

$$4\pi \int_0^\infty \chi_\nu [S_\nu - J_\nu] = 0 \qquad (35)$$

or, $J_\nu = S_\nu$, (7:49). Note that the radiative equilibrium assumption states that what is created within a volume is destroyed in this volume implies that the total radiation flux within a volume must be constant, or

$$\frac{1}{r^2} \frac{\partial(r^2 H\nu)}{\partial r} = \chi_\nu (S_\nu - J_\nu) = 0$$

or

$$r^2 H_\nu = \text{constant}: \; 4\pi r^2 H_\nu = F_\nu = \text{constant} \qquad (36)$$

The Grey Atmosphere. A fundamental example for the analysis of stellar atmospheres, and the specific case of study of this thesis, is the investigation of the grey atmosphere. The grey atmosphere problem is appropriate for the study of solutions to the transfer equation because the assumptions which are entailed are such that the solution of the equation becomes independent of the nature of the material itself. In addition, the problem introduces the aspect of radiative equilibrium, which may then be expanded to more realistic cases of non-grey, non-static problems.

The crux of the grey atmosphere problem is that the

opacity of the material is independent of frequency, thus $\chi_\nu = \chi$ (a constant). Further, integrating all quantities over frequency such that

$$\chi = \int_o^\infty \chi_\nu \, d_\nu \tag{37}$$

where $x_\nu = I_\nu, J_\nu, S_\nu$, etc., the transfer equation takes on the form

$$\mu \frac{\partial I}{\partial r} + \frac{(1-\mu^2)}{r} \frac{\partial I}{\partial \mu} = \chi (S - J) \tag{38}$$

Summary. Before finally moving on to the specifics of the ray-integration technique, a summary of the assumptions and approximations of this section is given below.

Table IV

Radiative Equilibrium and Grey Atmosphere Assumptions

Assumption	Statement	Result
Radiative Equilibrium	$J = S$	$4\pi r^2 H$ = constant
Grey Atmosphere	$\chi = \chi_\nu$	I, J, H, K, S are frequency independent

Table V

Variable Eddington Factors

Ratio	Symbol	Diffusion Limit Approximation	Streaming Approximation
K/J	f_k	$f_k \rightarrow \frac{1}{3}$	$f_k \rightarrow 1$
H/J	f_H	$f_H \rightarrow 0$	$f_H \rightarrow 1$

III. The Ray-Integration Technique

Having developed the basic theory of radiation transport, attention is now turned to the actual solution of the grey atmosphere problem via the ray-integration technique.

Statement of the Problem

To reiterate, the purpose of this thesis is to explore a method of solution to the spherical coordinate form of the equation of radiative transfer, specifically for the grey atmosphere, steady state problem. This method of solution is called the ray-integration technique. As the name implies, the gist of this method is the solution of the transfer equation along lines of intensity, called rays. The rays are divided into small length segments, ds, and the transfer equation solved each segment. The solutions are then integrated numerically over the entire ray. A step-by-step development of this method is described in the next section.

Development of the Method

To begin an explanation of this method, first, imagine a spherical plasma having a central region which produces copious amounts of photons. A physical analogy of this would be the interior of a star where subatomic interactions result in large amounts of radiation output. In this region, radiation field is very dense and the mean free paths of the photons are very small. In other words, the optical depth is very large. Here the diffusion limit is valid. Now imagine

that this interior, very dense region is surrounded by an extended envelope of material that is considerably less opaque to photons, i.e., a region where the photons mean free path is considerably longer. This region can be likened to the atmosphere of a star. It is through this atomosphere region that the radiation is transported from the interior to, and out of, the surface of the plasma body.

The location of any point within this sphere is defined by specifying its radial distance, r, from the center and the longitudinal and azimuthal angles, (α and β) made with the axis' of the sphere, see Figure 2.

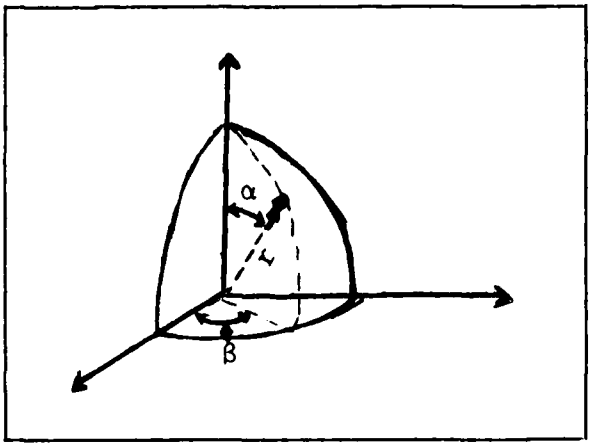

Figure 2

Location of a Point on a Sphere

Now, subdivide the sphere into a series of concentric shells and imagine a ray of photons passing through the sphere tangent to one of the shells. The position of the ray at that tangent point is now further defined by specifying the local or directional, longitudinal and azimuthal angles made with

respect to the normal to the surface. See Figure 3.

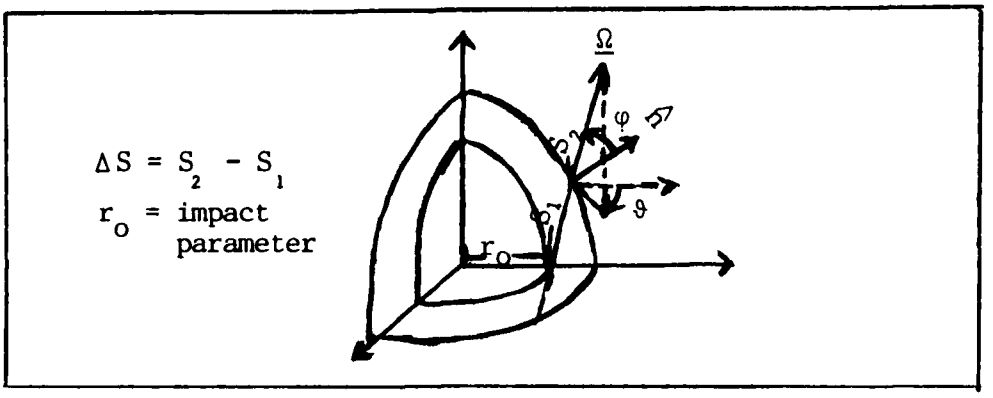

Figure 3a.

Directional Angles of a Ray Passing Through a Sphere

Thus, in general, the intensity measured at any point within the sphere is a function of the radial distance, r, and the four angles α, β, ϑ and φ. However, for the one-dimensional case, we are considering the intensity is independent of angles α, β and ϑ . In other words,

$$I(r,\alpha,\beta,\vartheta,\varphi) = I(r,\varphi) \tag{39}$$

Now, let's examine the φ relationship. Imagine that the ray of photons has a length s and an elemental length Δs between to radii. If this distance is sufficiently small, then $\Delta s \approx ds$. Similarly, $\Delta r \approx dr$. See Figure 3b.

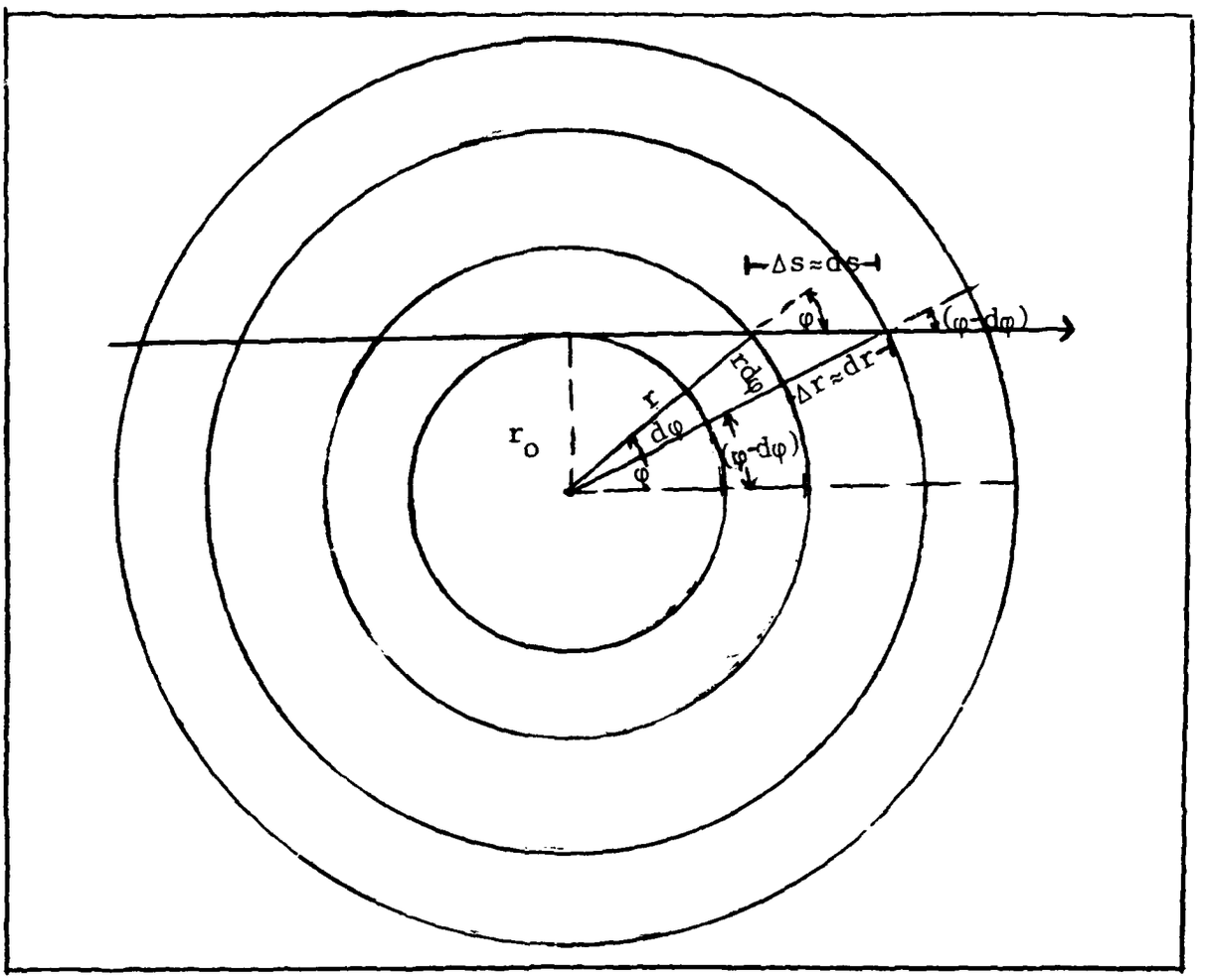

Figure 3b

Coordinates of a Ray Passing Through a Sphere.

From the geometry, it is clear that

$$\cos(\varphi - d\varphi) \approx \cos(\varphi) = \frac{dr}{ds} \tag{42}$$

Further, note that

$$(dr)^2 + (-rd\varphi)^2 \approx ds^2 \tag{43}$$

or

$$\frac{d\varphi}{ds} = \frac{-\sin(\varphi)}{r} \tag{44}$$

Relating these relations to the directional derivative used in solving the transfer equation, we have

$$\underline{\Omega} \cdot \nabla I = \frac{\partial I}{\partial s} = \frac{\partial r}{\partial s}\frac{\partial I}{\partial r} + \frac{\partial \varphi}{\partial s}\frac{\varphi I}{\partial \varphi}$$

$$= \cos(\varphi)\frac{\partial I}{\partial r} - \frac{\sin(\varphi)}{r}\frac{\partial I}{\partial \varphi}$$

$$= \frac{\partial I}{\partial r} + \frac{(1-\mu^2)}{r}\frac{\partial I}{\partial \mu} \tag{45}$$

where $\mu = \cos(\varphi)$. The above is just the relation that was simply stated in the last chapter. Recall that the solution to the transfer equation is

$$I(\tau) = I(o)\, e^{-\tau} + \int^{\tau} S(\tau)\, e^{(\tau' - \tau)}\, d\tau' \tag{23}$$

which, for a differential length of ray, ds, and using $d\tau = \chi(s)ds$, $\tau = \int_{s_1}^{s_2} \chi(s')\, ds'$, is

$$I(s_2) = I(s_1)\, e^{-\int_{s_1}^{s_2} \chi(s) ds'} + \int_{s_1}^{s_2} S(s')\, \chi(s')\, ds'\, e^{-\int_{s'}^{s_2} \chi(s'') ds''} \tag{46}$$

The object of the ray-integration technique is to solve the above equation for each length of ray, ds, between two radii and to add the solutions for each increment in order to find the solution for the intensity along the entire ray; in other words, to numerically "integrate" the intensity over the entire ray.

IV. Numerical Solutions

Numerical solutions to the transfer equation via the ray-integration technique were implemented explicitly by computer code. In this section, the numerical methods, the logic behind them and the differencing schemes produced are detailed.

Geometry Dependent Variables

Radial Mesh. The first task in solving a geometry dependent problem is to define the geometry dependent variables. First of these are those variables defining the physical size of the plasma and the number and spacing of radii which the sphere is divided into; in other words, the radial mesh.

The size of the sphere is defined indirectly by inputting the number and spacing of radii. These values are essentially arbitrary and can be scaled up to the size of a stellar body or down to a small spherical plasma. The form of the radial mesh is also arbitrary. That is, an evenly spaced mesh can be used as reasonably as a logarithmic scheme, or even a completely random spacing. An example of how a five radii, evenly spaced mesh might look is illustrated by Figure 4. The mesh is indexed such that jn is the total number of radii, with the first radius being defined as zero. That is, in terms of the example, jn = 5, r(1) = 0.0, r(2) = 0.005 m, etc., through r(5) = 0.02 m.

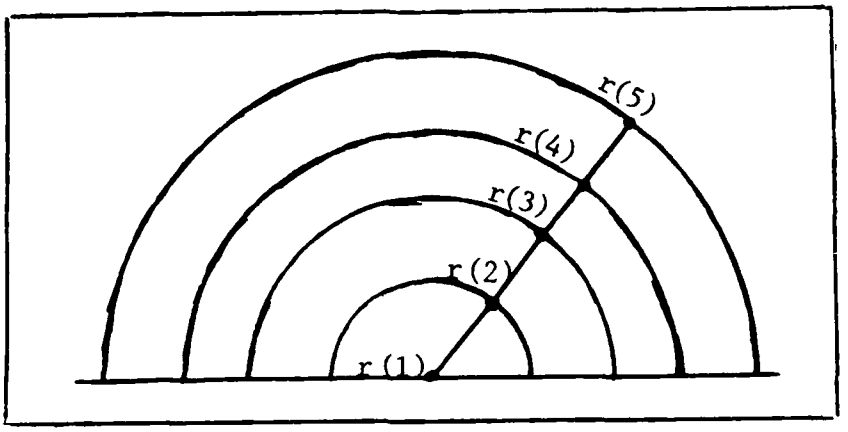

Figure 4

Example of an Evenly-Spaced Radius Mesh

Angular Mesh. Refer back to Figure 4. Note that there is an angle φ made with the radius normal for each ray that passes through the sphere. If many rays pass through the sphere, all at different φ angles, then there will be a distribution of angles for each radius so that each radius has an angular mesh which looks like Figure 5.

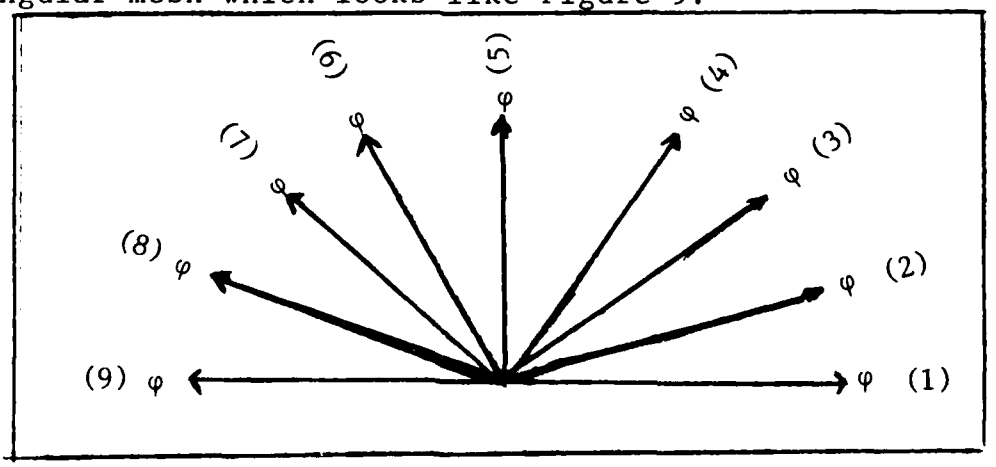

Figure 5

Angular Mesh of an Evenly-Spaced, Five-Radius Sphere

We see that each radius point has as many angles associated with it as rays that pass tangent to it. If we define the rays to be symmetric about $\mu = 0$, then only half the number of angles which exist need to be generated, since the angles on one side of the centerline are just the negative of their mirror mate.

Generation of Angular Weights. Recall that the quantities which are used to analyze a spherical radiation field include the angular moments of intensity, J, H, and K. Take for example the moment J whose equation is

$$J = \frac{1}{2} \int_{\mu-}^{\mu+} I(\mu)\, d\mu \tag{47}$$

Where $\mu+$ is the angle at the beginning of the ds interval and $\mu-$ is the angle at the end. This integral equation must be given a numerical equivalent for solution by computer code. This was accomplished by the method of Gaussian quadrature, such that

$$\frac{1}{2} \int_{\mu-}^{\mu+} I(\mu)\, d\mu \approx \sum_{k=1}^{3} I(\mu)\, w_k \tag{48}$$

where w are the numerical weights which allow the summation to approximate the integral (see Appendix A for an explanation of Gaussian quadrature). As before, I is the intensity on the Δs interval. Note that intensity, I, must be given a numerical representation as well. Thus far, the intensity

has been defined in terms of energy flow, but no particular polynomial representation has been presented. There are actually a number of ways in which the intensity can be expanded, all with equally varied degrees of accuracy. Many forms of polynomial expansion were attempted in the solution of this problem. It was found, however, that a second degree Legendre polynomial expansion gave the greatest degree of accuracy. This expansion is

$$I(\mu) = a + b\mu + \quad (3\mu^2 - 1) \tag{49}$$

Thus, equations (46) and (47) yield the expression

$$\sum_{k=1}^{3} w_k \, I(\mu) \approx a(\mu_+ - \mu_-) + \frac{b}{2}(\mu_+^{\,2} - \mu_-^{\,2}) + \frac{c}{2}(\mu_+^{\,3} + \mu_-^{\,3} - \mu_+ + \mu_-) \tag{50}$$

The weights are found three at a time by solution of the resulting matrix equation

$$\begin{bmatrix} 1 & 1 & 1 \\ \mu_- & \mu_o & \mu_+ \\ \dfrac{3\mu_-^{\,2}-1}{2} & \dfrac{3\mu_o^{\,2}-1}{2} & \dfrac{3\mu_+^{\,2}-1}{2} \end{bmatrix} \begin{bmatrix} w_- \\ w_o \\ w_+ \end{bmatrix} = \begin{bmatrix} (\mu_+ - \mu_-) \\ \left(\dfrac{\mu_+^{\,2} - \mu^2}{2}\right) \\ \left(\dfrac{\mu_+^{\,3} - \mu_-^{\,3} - \mu_+ + \mu_-}{2}\right) \end{bmatrix}$$

B. Material Properties

Now that the geometrical properties have been developed, the physical characteristics of the radiation field, some of which are explicitly angular dependent, can also be derived. In this section, then, the material properties of opacity and emissivity (in the form of the source function) and the derived quantity of optical depth are developed in their difference form.

Opacity. Opacity of an extended atmosphere is a strong function of radius. There are numerous methods used to define this dependency (see for an example Reference 2). The discretization formula chosen in this study was a cubic spline fit, of the form

$$\chi\,(r(j)) = a_1 + a_2\, r(j) + a_3\, r(j)^2 \qquad (51)$$

where a1, a2, and a3 are constants chosen to mimic the nature of the plasma being analyzed. The validity of this formula was established by Dr. George Nickel in his cylindrical version of the ray integration technique.

The Optical Depth. From knowledge of the opacity, the optical depth at the tangent points can be derived. Recall that the relationship between the two is

$$\tau = \int_{s_1}^{s_2} \chi\,(s')\, ds' \qquad (52)$$

Using the geometry established where

$$\frac{ds}{dr} = \sec(\varphi) = \frac{r}{\sqrt{r^2-r_o^2}} \tag{53}$$

the integral in ds can be reduced to an integral in dr by

$$\tau = \sum_{i=o}^{3} a_i \int_{r_1}^{r_2} \frac{r(j+1)dr}{\sqrt{r^2 - r_o^2}} = \sum_{i=o}^{3} a_i \sum_{i=o}^{4} P_i \tag{54}$$

The integral is solved by the exact integration formula taken from Reference 1, where

$$P_1 = \sqrt{r_2^2-r_o^2} \quad - \quad \sqrt{r_1^2-r_o^2}$$

$$P_2 = r_2 \sqrt{r_2^2-r_o^2} \; -r_o \sqrt{r_1^2-r_o^2} \; + \frac{1}{2} \left(\ln(\sqrt{r_2^2-r_o^2} \; -\sqrt{r_1^3-r_o^2})\right)$$

$$P_3 = \left((r_2^2 + 2r_o^2) \sqrt{r_2^2-r_o^2} \; -r_1^2 + 2r_o^2 \sqrt{r_1^2-r_o^2}\right)/3$$

$$P_4 = \left((r_2 \sqrt{r_2^2 + 2r_o^2}\,) \quad (r_2^2 + 1.5\, r_o^2)\right)/4$$

$$+ \frac{3}{8} \left(r_o^4 \ln \sqrt{r_2^2-r_o^2}\right)$$

$$- \left((r_1 \sqrt{r_1^2 + 2r_o^2}) \; (r_1^2 + 1.5r_o^2)\right)/4$$

$$- \frac{3}{8} \left(r_o \quad \ln \sqrt{r_1^2-r_o^2}\right) \tag{55}$$

The Source Function. The last material property necessary for the solution of the transfer equation is the emissivity. This quantity appears in the transfer equation in the form of the source function, S.

It is assumed that the source function, like opacity, is a function of radius. The exact variation is not as simple to predict as with the opacity. A more complex relationship exists. Traditionally, an estimate of the source function is made based on observable quantities. However, a method of refining this initial estimate has been produced and is the fundamental quantity which makes the ray-integration technique both unique and eminently practical. In this section, the "first guess" source function estimate is derived and then, from it, the specific solution.

Initial Estimate of the Source Function. The source function of a system, such as a stellar body in the depths of space or a small plasma confined in a magnetic field in a laboratory, can be inferred from the radiation flux emitted from a spherical body of radius r is just the rate of energy change per unit volume. Defining the quantity P (for power) as the rate of energy flow, along a distance r,

$$H = \frac{P}{4\pi r^2} \tag{56}$$

where H is the Eddington flux as defined in Chapter II. Now recall the first moment equation is

$$\frac{\partial K}{\partial r} + \frac{3K-J}{r} = -\chi H \qquad (29)$$

Assuming that the atmosphere is optically thick at r, then according to the Eddington approximation, 3K = J, and the second term vanishes. Further, making use of the assumption of radiative equilibrium, J = S, yields K = 1/3 S. Equation (29) becomes

$$\frac{1}{3}\frac{\partial s}{\partial r} = -\chi \frac{P}{4\pi r^2} \qquad (57)$$

Using a forward differencing scheme on the left hand side and assuming that the right hand side can be averaged such that

$$\frac{S(j+1) - S(j)}{r(j+1) - r(j)} = \frac{-3}{2} P \cdot \left(\frac{K(j)}{r(j)^2} + \frac{K(j+1)}{r(j+1)^2} \right) \qquad (58)$$

Solving through for S(j) yields

$$S(j) = S(j+1) + \frac{3}{2} (r(j+1) - r(j)) \cdot P \left(\frac{K(j)}{r(j)^2} + \frac{K(j+1)}{r(j+1)^2} \right) \qquad (59)$$

Note that this scheme can not be used at the outer boundary since in the steaming limit K = J, and the second term

does not vanish. Instead, another method must be developed to solve for the source function at that limit. This is done by the introduction of the extrapolated boundary. The extrapolated boundary is an imaginary boundary outside of the physical limit of the plasma system where the flux goes to zero. The extrapolated boundary is illustrated in Figure 6.

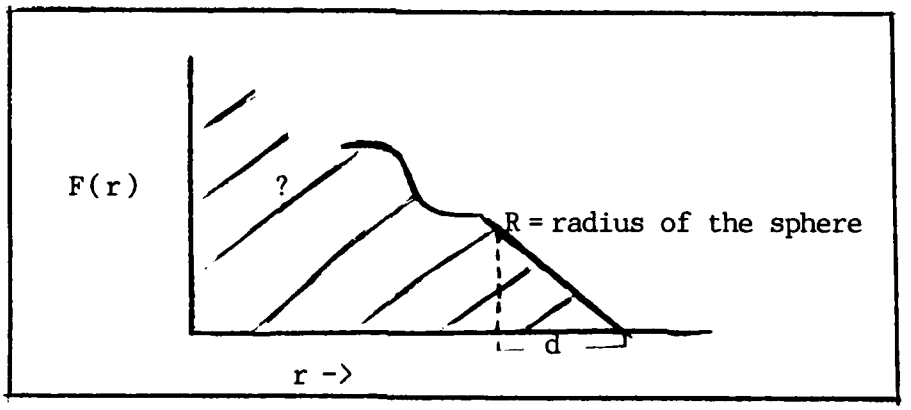

Figure 6

Flux at the Boundary (3:59)

The solution for the extrapolated boundary is outside the scope of this work, but is derived for both neutrons and photons in References 4 and 7. The solution is simply stated in this report as

$$r(jn) + d = \frac{2}{3} \frac{1}{\chi(jn)} \qquad (60)$$

where d = the extrapolated boundary, and r(jn) is the outer radius of the sphere. This outermost point is the classic

streaming limit, where by assumptions of Section II.C.3 H = J. Still assuming radiative equlibrium, J = S, thus by equation (57),

$$\frac{1}{3} S(jn)/(\frac{2}{3}\chi(jn)) = \frac{P}{4\pi r(jn)^2} \qquad (61)$$

This is the relation used to express the source function at the approximate physical boundry. The discrete form is

$$S(jn) = \frac{P}{2\pi} \frac{\chi(jn)}{r(jn)^2} \qquad (62)$$

Last in developing a source function for the sphere is the derivation of the innermost region. It is assumed that the centermost radius region contains a source which increases linearly with radius in the manner illustrated in Figure 7.

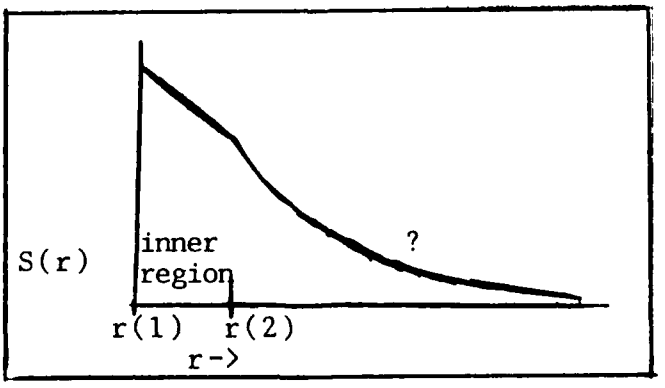

Figure 7

Radial Variation of the Source-Bearing Region.

Within the source region, the Eddington flux also varies. It continuously rises from H(o) to some value H(2), as illustrated by Figure 8.

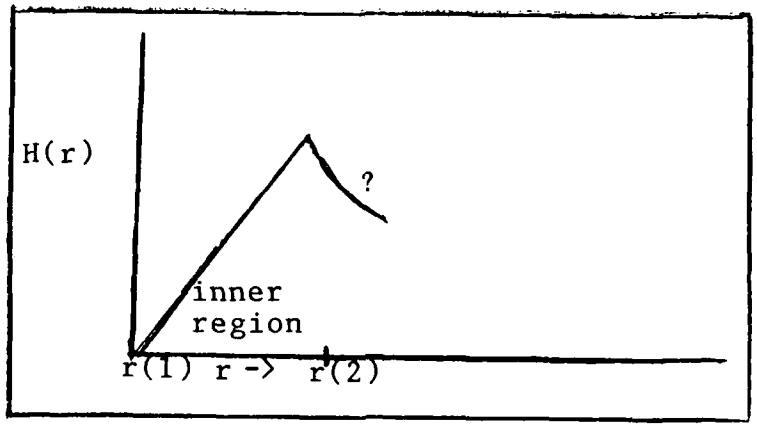

Figure 8

Radial Variation of the Eddington Flux.

The Eddington flux is thought to vary linearly within this region. The solution of the first moment equation, thus, gives

$$\frac{1}{3}\left(\frac{S(2)-S(1)}{r(2)-r(1)}\right)=\frac{1}{2}\cdot\left(\chi(1)\,H(1)+\chi(2)\,H(2)\right) \qquad (63)$$

Differencing the above yields

$$S(1)=S(2)+\frac{3}{8}\cdot\left(\chi(2)\cdot\frac{P}{4\pi r(2)^2}\right) \qquad (64)$$

Refinement of the Source Function Estimate. Using the reasoning outlined above, a value for the source can be estimated at each point on the radius mesh. However, recall the solution to the transfer equation involved an integral of the source over the length of the ray. This equation is

$$I(s_2) = I(s_1)\, e^{-\int_{s_1}^{s_2} \chi(s)ds'} + \int_{s_1}^{s_2} S(s')\,\chi(s')\,ds'\, e^{-\int_{s'}^{s_2} \chi(s'')ds''} \qquad (65)$$

To avoid having to solve this rather cumbersome integral equation, we create an "equivalent source function" which we will call S*, such that equation (65) can be made into

$$I(s_2) = I(s_1)\, e^{-\tau} + S^* (1 - e^{-\tau})$$

Development of the S* Function. To establish the S* function, first consider the radius segment shown in Figure 9.

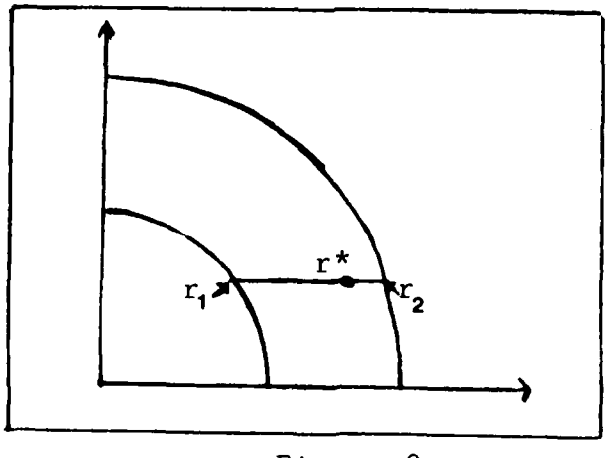

Figure 9

Radial Segment Showing Position of r*.

The distance r* is defined as the spatial distance along the ray of length $S_2 - S_1$, at which the equivalent source function S* exists. Said in other words, at r*, the source function has a value S*, which, if used in the solution of the transfer equation, reduces (65) to (66). Assuming that the source function varies linearly over the interval s_2 to s_1, the function S* can be approximated as

$$S^* = S_1\left(\frac{r_2 - r(s)}{r_2 - r_1}\right) + S_2\left(\frac{r(s) - r_1}{r_2 - r_1}\right) \tag{67}$$

Substituting this into (66) yields

$$I(S_2) = I(s_1)\, e^{-\int_{s_1}^{s_2} \chi(s')ds'} + \left(\frac{S_1 r_2 - S_2 r_1}{r_2 - r_1}\right) \int_{s_1}^{s_2} ds' \chi(s')\, e^{\int_{s_1}^{s_2} \chi(s'')ds''} \tag{68}$$

$$+ \frac{S_2 - S_1}{r_2 - r_1} \int_{s_1}^{s_2} ds'\, \chi(s')\, r(s')\, e^{\int_{s_1}^{s_2} \chi(s'')\, ds''}$$

Note that the first integral term can be easily reduced to

$$\frac{S_1 r_2 - S_2 r_1}{r_2 - r_1}\left(1 - e^{-\tau}\right) \quad \text{where} \quad \tau = \int_{s'}^{s_2} \chi(s'')\, ds'' \tag{69}$$

The second integral term can also be reduced by defining r* as

$$r^* = \frac{\int_{s_1}^{s_2} ds'\ (s')\, e^{\int_{s_1}^{s_2} \chi(s'')ds''}}{1 - e^{-\tau}} = \frac{\int_0^{\tau} d\tau\, r(\tau)\, e^{-\tau}}{1 - e^{-\tau}}$$

Using (69) and (70) in (66) gives

$$I(s_2) = I(s_1)\, e^{-\tau} + (1-e^{-\tau})\left(\frac{S_1 r_2 - S_2 r_1}{r_2 - r_1}\right) + (1-e^{-\tau})\left(r^* \frac{S_2 - S_1}{r_2 - r_1}\right) \quad (71)$$

or

$$I(s_2) = I(s_1)\, e^{-\tau} + (1-e^{-\tau})\left(S_1 \frac{r_2 - r^*}{r_2 - r_1} + S_2 \frac{r^* - r_1}{r_2 - r_1}\right) \quad (72)$$

Thus, we have transformed the messy integral of equation (65) into the much neater, and numerically convenient, form of equation (66).

$$I(s_2) = I(s_1)\, e^{-\tau} + S^* (1-e^{-\tau}) \quad (73)$$

The difficulty now lies in the solution to the r* integral. This is done via the method of cubic splines leading to incomplete gamma functions. The definition of the method of cubic spline interpolation is found in Appendix B. Its application to generation of the r* function is given below.

Development of the r* Function. Recall that the r* function is

$$r^* = \frac{\int_0^\tau r(\tau')\, e^{-\tau}\, d\tau}{1 - e^{-\tau}} \quad (74)$$

First, the interpolatory function is fitted to the r (τ)

polynomial which has the values of

$$r(o) = r_1$$

$$r(\tau) = r_2$$

$$\left.\frac{dr}{d\tau}\right|_o = 1/\left(\frac{d\tau}{dr}\right) = \left(\sqrt{r_2^2 - r_o^2}\right) / \left(r_2 \chi(r)\right)$$

$$\left.\frac{dr}{d\tau}\right|_\tau = \left(\sqrt{r_2^2 - r_o^2}\right) / \left(r_o \chi(r_o)\right) \tag{75}$$

With these values and slopes, $r(\tau)$ is of the form

$$r(\tau) = \sum_{j=o}^{3} b_j \tau^j \tag{76}$$

Where,

$$b_o = r_2$$

$$b_1 = \left.\frac{dr}{d\tau}\right|_2$$

$$b_2 = \frac{3(r_1 - r_2)}{\tau^2} + \frac{\left.\frac{dr}{d\tau}\right|_1 + 2\left.\frac{dr}{d\tau}\right|_2}{\tau}$$

$$b = \frac{2(r_2 - r_1)}{\tau^3} + \frac{\left.\frac{dr}{d\tau}\right|_1 + \left.\frac{dr}{d\tau}\right|_2}{\tau^2} \tag{77}$$

so that

$$r^* = \sum_{j=o}^{3} b_j \int_o^\tau \tau^j e^{-\tau} d\tau' \tag{78}$$

Some care must be taken when evaluating these incomplete gamma functions at small argument, since large subtraction errors develop. For example,

$$\Gamma_3(\tau) = \int_0^\tau \tau'^3 e^{-\tau'} d\tau' = 6 - 6\left(1 + \tau + \frac{1}{2}\tau^2 + \frac{1}{6}\tau^3\right) e^{-\tau}$$

As $\tau \to \infty$, $\Gamma \to 3!$, as it should. Clearly, though, when $\tau \ll 1$, a significant problem develops in that

$$\Gamma_3(\tau) \approx \frac{1}{4}\tau^4 \text{ (ignoring } e^{-\tau})$$

If τ is 10^{-3}, for example, Γ_3 is 2.5×10^{-13}. Clearly, the difference between 6 and $6(1\pm10^{-3} + 1/2\times10^{-6} + 1/6\times10)^{-9}e^{-\tau}$ will tax the decimal places of a CRAY in single precision.

However, the following prescription gives good accuracy over the entire range.

Let Psmall = $1/4\,\tau^4 - 1/5\,\tau^4 + 1/12\,\tau^6$

$$\text{Pbig} = 6 - (1.02228\tau^3 + 3.00939\tau^2 + 5.002488\tau + 5.1244)e^{-\tau}$$

Then $$\Gamma_3(\tau) = \frac{\text{Psmall} * \text{Pbig}}{\text{Psmall} + \text{Pbig}}$$

The lower terms are found by downward recursion such that

$$\Gamma_2(\tau) = \frac{1}{3}\left(\Gamma_3(\tau) + \tau^3 e^{-\tau}\right)$$

$$\Gamma_1(\tau) = \frac{1}{2}\left(\Gamma_2(\tau) + \tau^2 e^{-\tau}\right)$$

$$\Gamma_0(\tau) = \Gamma_1(\tau) + \tau e^{-\tau}$$

(Reference 8) Thus, the r* integral is solved by generating the incomplete gamma function in the method described above at each ds interval.

Numerical Solution to the Transfer Equation

Now, all physical parameters of the plasma have been presented: the dimensions, the angular variables and the material properties. With this information on hand, the intensity (and, subsequently, its moments), can be solved for. Recall, however, that the material properties input are only approximate. Even the S* function is based on an approximate "first guess" source function, and thus has limited, albeit improved, accuracy. Consequently, the moments J, H, and K share the limited accuracy of I. The repair for this inaccuracy is done via iteration.

In this section, the numerical form of the solution to the transfer equation, that is, the derivation of the value for I at each radius, is presented. Following this, the calculation of the moments of intensity is expounded upon. Last is presented the iteration techniques used to force the condition of radiative equilibrium, thereby providing the correct solution of the problem.

Solution of the Transfer Equation. Using the generated source function S*, the transfer equation reduces in terms of the radius mesh to

$$I(j+1) = I(j)e^{-\tau(j+1)} + S^* (1-e^{-\tau(j+1)}) \qquad (79)$$

where, I(J+1) is the intensity at the last ds interval. In previous chapters, we have discussed passing rays through a sphere, but have not defined the order in which this is done. Figure 10 shows the order of rays which are evaluated for a five radius radial mesh.

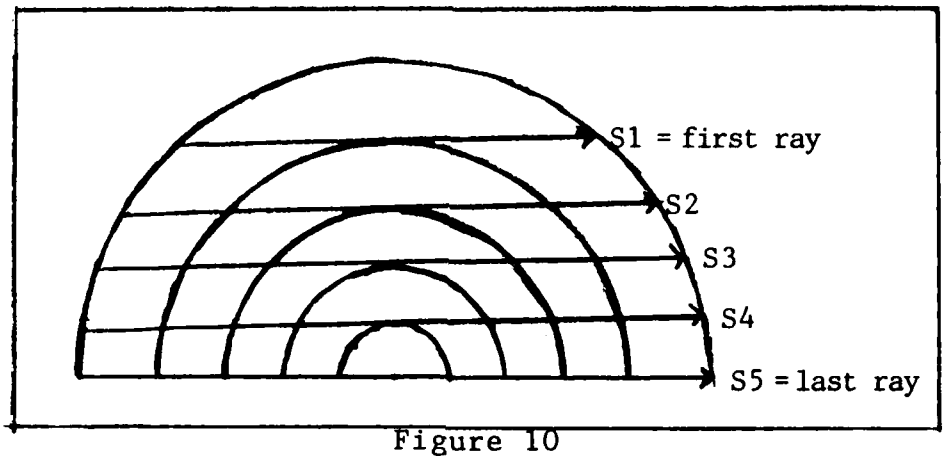

Figure 10

Order of Rays of Intensity Passing Through a Sphere

Beginning with the outermost ray, S1, the equation is solved for each segment along the ray until the entire ray is summed over, or integrated.

In this example, there are five radii. The outer ray has two ds segments to the ray. The next ray has four segments. The last has eight. Beginning with ray one, I(5) is solved from

$$I(5) = I(6)e^{-\tau(6)} + S^* (1 - e^{-\tau(6)}) \qquad (80)$$

where I(6) =0. Then I(4) is

$$I(4) = I(5)e^{-(5)} + S^* (1 - e^{-(5)}) \qquad (81)$$

Again I(5) is solved for by

$$I(5) = I(4)e^{-(4)} + S^* (1 - e^{-(4)}) \qquad (82)$$

Integration over ray two is then done such that

$$--I(5) = I(6)e^{-(6)} + S^* (1 - e^{-(6)})$$

$$--I(4) = I(5)e^{-(5)} + S^* (1 - e^{-(5)})$$

$$--I(3) = I(4)e^{-(4)} + S^* (1 - e^{-(4)})$$

etc., to

$$--I(5) = I(4)e^{-(4)} + S^* (1 - e^{-(4)})$$

The process is repeated, ray by ray, until the center ray is integrated.

Solution of the Moments of Intensity. By solving for the intensity at each radius for each ray, we are simply solving for the intensity at each angle on the radius mesh. The moments of intensity are then found by numerically integration, using these solutions. Or

$$J(r) = \sum_{\mu=-1}^{\mu=+1} I(r,\mu)\, w_k$$

$$H(r) = \sum_{\mu=-1}^{\mu=+1} I(r,\mu)\, w_k$$

$$K(r) = \sum_{\mu=-1}^{\mu=+1} I(r,\mu)\, w_k$$

where w_k are the weights for each angle and I is the value of intensity solved for at each angle (ray interception point).

Iteration of the Solution. As previously stated, the solution to the transfer equation has a limited accuracy as solved above, due to the initial crudeness of estimates of the material properties. The source function approximates, but does not guarantee, radiative equilibrium. However, knowing J and S at each radius point equilibrium can be forced by successive iteration. The method of iteration depends implicitly on the optical thickness of the material. There are two commonly accepted schemes of iteration, the Lambda iteration scheme for the optically thin case and the Unsold iteration scheme for the optically thick case.

Lambda Iteration Scheme for the Optically Thin Atmosphere. The Lambda iteration is essentially the statement of radiative equilibrium. That is, the source at each radius point is simply replaced by the mean intensity calculated by the ray-integration scheme. Analytically,

$$S(j) = J(j) \tag{83}$$

It would seem at first glance that this is sufficient to establish radiative equilibrium; however, it is not over a wide variety of ranges. As stated by Mihalis in Reference 7, "In principle, successive applications of the (Lambda iteration scheme) should improve the solution, and, eventually, produce the exact solution. ...In practice, however, the convergence

is too slow to be of any value, if the effective range ... is of order = 1, so errors at large depth are removed only 'infinitely slowly.'" (7:62).

The Unsold Iteration Scheme for Optically Thick Atmospheres. As a result of the Lambda iteration being inappropriate to use for optically thick atmospheres, another scheme must be used. This second method is called the Unsold iteration, after its creator (Ref 7). The Unsold iteration, is developed from the first order moment equation, which is

$$\frac{\partial K}{\partial r} + \frac{3K-J}{r} = -\chi H \tag{27}$$

Introducing an integrating factor, q, known as the sphericity function, the above equation can be reduced to

$$\frac{1}{q}\frac{d(qK)}{dq} = -\chi H \tag{84}$$

where

$$\frac{K}{q}\frac{dq}{dr} = \frac{3K-J}{r} \tag{85}$$

Differencing this yields

$$q(j+1)\,K(j+1) - q(j)\,K(j) = -\frac{1}{2}\left\{\left[\chi(j)q(j)H(j) + \chi(j+1)q(j+1)H(j+1)\right] \cdot \left[(r(j+1) - r(j))\right]\right\} \tag{86}$$

or

$$q(j+1)\left(\chi(j+1)+\frac{1}{2}(r(j+1)-r(j)\chi(j+1)H(j+1)\right) = q(j)\left(\chi(j)-\frac{1}{2}\right.$$
$$\left.\cdot(r(j+1)-r(j))\chi(j)H(j)\right) \quad (87)$$

We then assume that deviation from the "true" values of the moments vary linearly such that

$$\frac{1}{q}\frac{d(qf_k\Delta J)}{dr} = -\chi(\Delta H) \quad (88)$$

where $f_k = \Delta K/\Delta J$, $\Delta H = (P/4\pi r^2)-H_{calc}$, $\Delta J = J_{ex} - J_{calc}$. Note that for radiative equalibrium J = S. We substitute the q's calculated into the previous equation and solve through for $J_{exact}(=S_{exact})$, which yields

$$S(j) = \left[J(j) - \frac{(r(j+1)-r(j)K(j)H(j)}{2f(j)}\right] + \frac{(r(j+1)-r(j))\ P}{2\ f(j)\ 4\pi r(j)^2} \quad (89)$$
$$\left[\frac{S(j+1)(PJ(j+1)/(4\pi r(j)^2H(j))+\frac{1}{2}(r(j+1)-r(j))\chi(j+1)H(j+1)}{f(j)+J(j+1)+\frac{1}{2}(r(j+1)-r(j))\chi(j+1)+H(j+1)}\right]$$

This is a self consistent equation which, in the limit of $\Delta H=0$, produces

$$S(j) = J(j) \quad (90)$$

This value can now be used to generate a new, more accurate S* function and hence bring the answer closer to the correct equilibrium value. This iteration solution brings about a stable solution within just a few iterations.

Solution of the Moments Equations

Although solution of the moments equations will not yield any new information in terms of the intensity through the sphere, there is a usefulness in solving for these equations numerically. That is, once values for the intensity, source function, J and K have been solved for they can be substituted into the moments equations. The moments equations are now solved for H and the value of H compared with that generated by the integration of rays. This, then, is an excellent check on the relative accuracies of the values calculated as well as an informative look at relative accuracy of the moments equations as compared to each other. For the purpose of completion, the differization of the moments equations are reproduced below.

The Zero'th Order Moment Equation. The formulation for the zero'th moment equation is

$$\frac{1}{r^2}\frac{\partial(r^2H)}{\partial r} = \chi(S - J) \tag{91}$$

Using the backward difference method on the term on the left hand side, and averaging the right hand side, yields

$$\frac{1}{r(j+1)^2-r(j)^2}\left(\frac{r(j)^2H(j)}{r(j)^2} - \frac{r(j-1)^2H(j-1)}{r(j-1)^2}\right) = \frac{1}{2}\Big(\chi(j)(S(j)-J(j)) + \chi(j+1)(S(j-1)-J(j-1))\Big) \tag{92}$$

H(0) is not solved for in this manner, but is defined as identically equal to zero for reasons outlined in Chapter II.

The First Order Moment Equation. In a like manner, the first order moment equation

$$\frac{\partial K}{\partial r} + \frac{3K-J}{r} = -\chi H \tag{93}$$

is given the numerical equivalent

$$\frac{K(j+1)-K(j)}{r(j+1)-r(j)} + \frac{1}{2}\left[\frac{3K(j)-J(j)}{r(j)} \quad \frac{3K(j+1)-J(j+1)}{r(j+1)}\right] = -\frac{1}{2}\left[\chi(j)H(j) + \chi(j+1)H(j+1)\right] \tag{94}$$

V. Computer Code Logic Flow

All of the elements of the ray-integration technique have now been discussed. In the first chapter, the basic definitions of the physical nature of radiation transport were examined. After which, an overview of the technique itself was provided along with a development of the logic which spawned it. And, in the last chapter, the numerical representations of the equations used in radiative transport were presented. The efforts to so differentiate the equations culminate in the creation of a computer code which in turn implements the ray-integration technique and produces an approximation for process of energy transport in the grey atmosphere problem.

The computer code that was used is listed in Appendix D. For convenience to the reader, the logic flow of the program is presented on the following page.

Table VI

Logic Flow for Computer Code

```
INPUT:
     -- OPACITY
     -- RADII
     -- POWER

CALCULATE:

     -- SOURCE FUNCTION
     -- ANGLES AND ANGULAR WEIGHTS
     -- OPTICAL DEPTH
     -- R* AND S*

FOR EACH RAY
     -- FOR EACH ds INTERVAL
          -- SOLVE TRANSFER EQ. FOR INTENSITY
          -- ACCUMULATE MOMENTS

NEXT RAY

SOLVE MOMENTS EQUATIONS

OUTPUT
     -- TOTAL RADIATION FLUX
     -- NET RADIATION FLUX
     -- SOURCE FUNCTION
     -- EDDINGTON FACTORS, f_k and f_H
     -- EDDINGTON FLUX FROM
          -- RAY-INTEGRATION TECHNIQUE
          -- ZERO AND FIRST MOMENT EQ.
```

VI. Results and Discussions

To meet the second objective of this thesis, verification of the ray-integration technique via computer code, the code stated in the last section was run with a variety of inputs. A sample of the results produced and a discussion of those results are presented in this section.

Case 1

To begin verification of the program, the code was run with a set of inputs approximating a sphere of outer radius equal to 0.011 meter, constant opacity, with an input for rate of energy change per radius of 6.28×10^{10} watts. The radius mesh used consisted of 22 radii, evenly spaced and having a width of 0.005 meters between mesh points. These values are essentially arbitrary, in that any physically valid set of data could be used. The output to the ray-integration program for this set of data is the total radiation flux ($4\pi r^2 H$), the opacity, the source function, S, the all-angle radiant intensity, J, and the moments ratios which include the Eddington factors f_k and f_H as well as the ratio J/S. The results are illustrated in Figures 11 through 14.

Consider, first, the total radiation flux. Theory predicts that the flux should rise from zero in the center to a constant value in the atmosphere and, due to the constraint of radiative equilibrium, remain constant throughout the sphere. Figure 11 shows that the program constructed follows

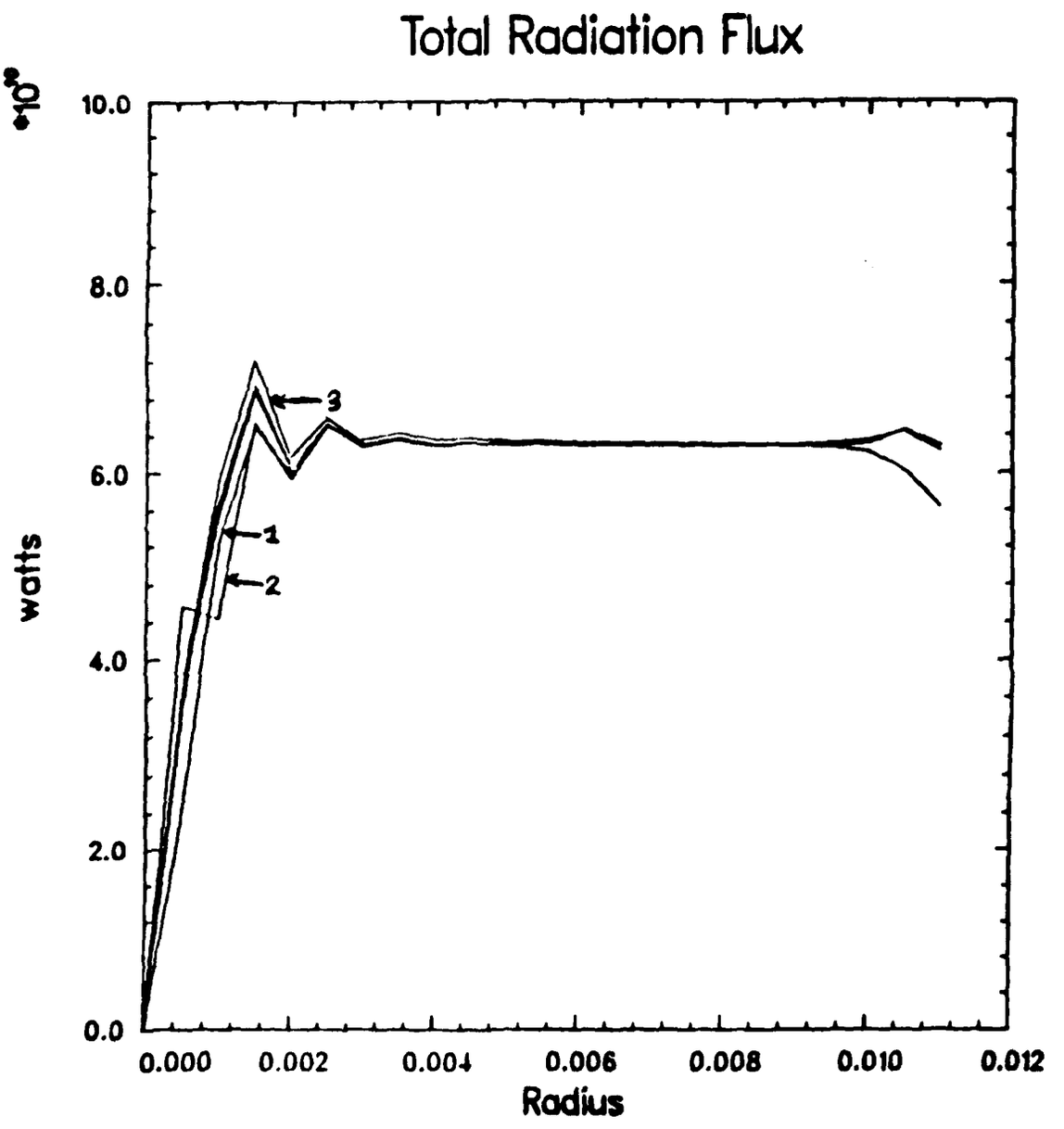

Figure 11

Total Radiation Flux (Case I)

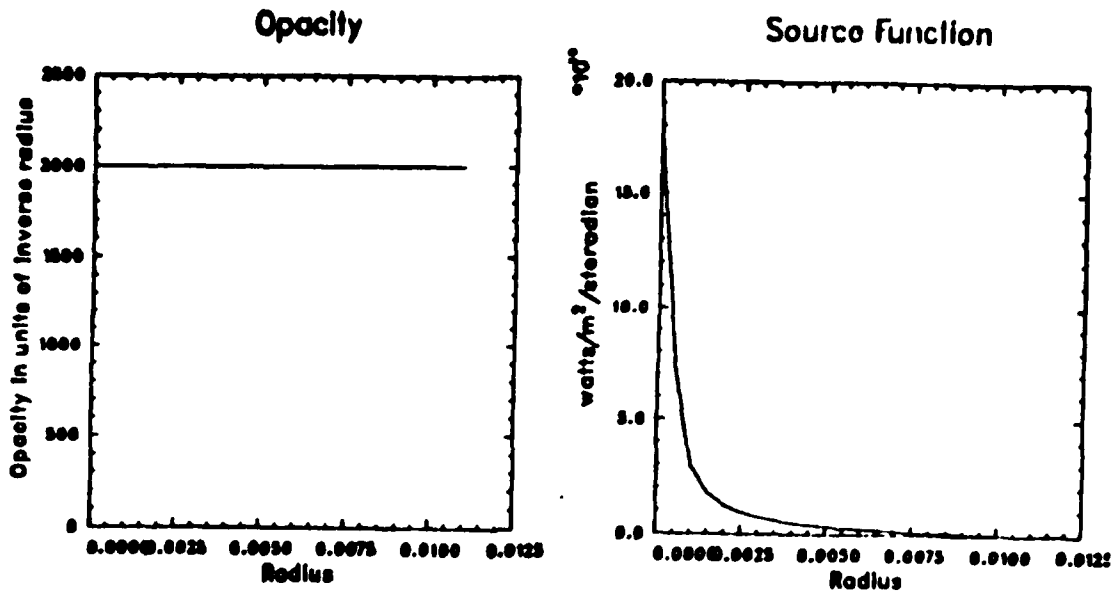

Figure 12

Opacity and Source Function (Case I)

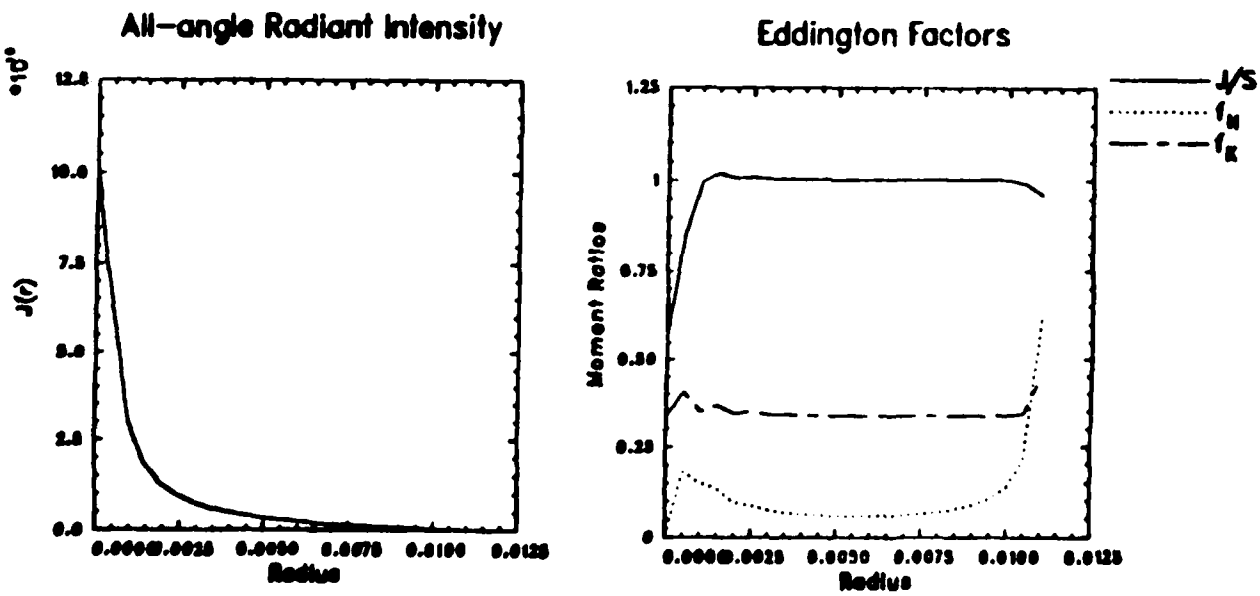

Figure 13

All-Angle Radiant Intensity and Eddington Factors (Case I)

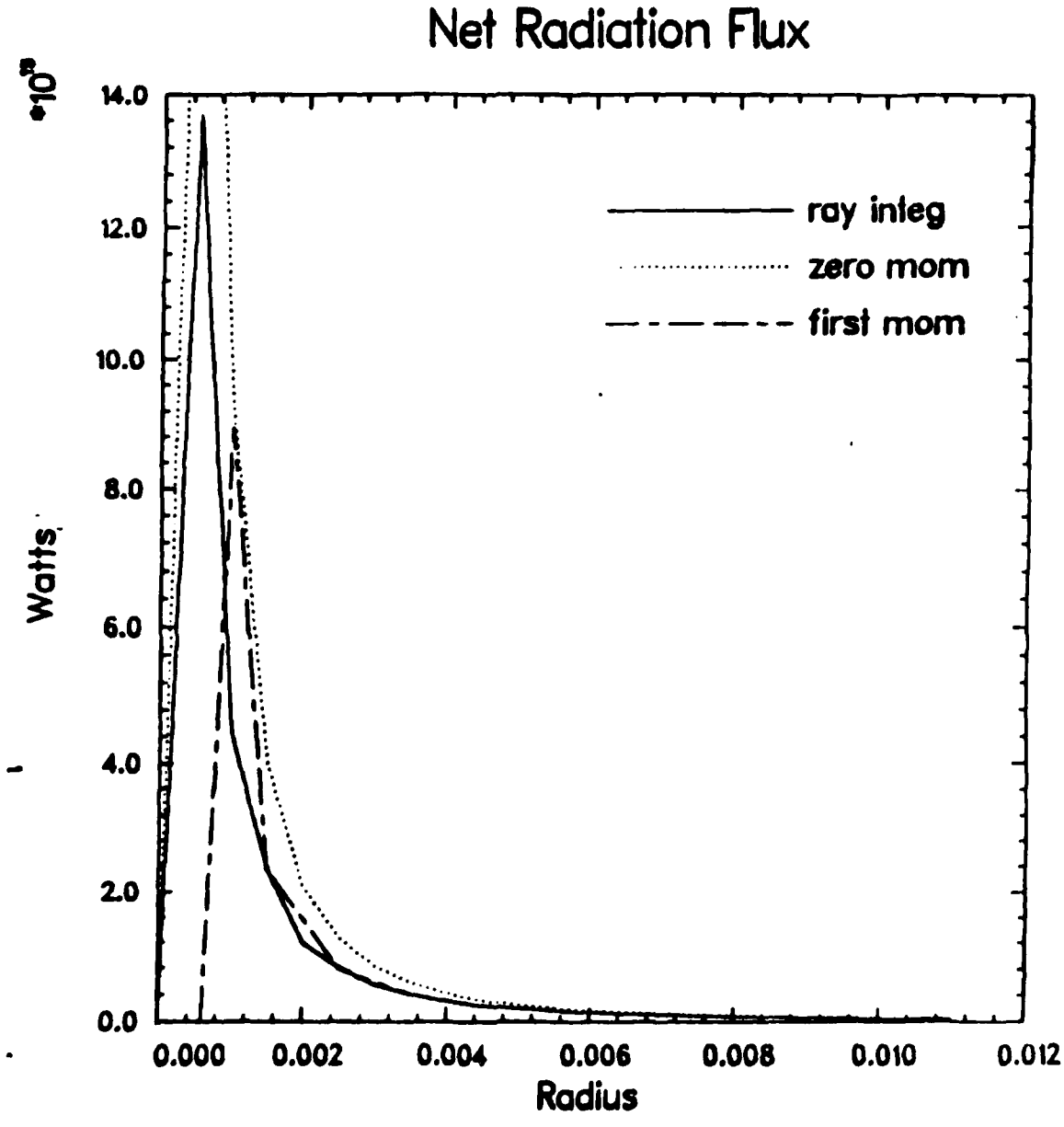

Figure 14

Net Radiation Flux (Case I)

this prediction reasonably well in the outer regions of the sphere, but produces some fluctuations in the innermost regions. Figure 11 shows the solution to the flux for 100 iterations. The first three iterations are identified on the graph by the numbers 1, 2 and 3. The solid line which is shown is the value to which the iteration converged. The fluctuations illustrated are not disturbing since, in any numerical analysis, slight inaccuracies are bound to occur. These could be due to round off error by the computer or to non-optimum approximations of the continuous functions involved. In this case, it is believed that the latter is responsible for the fluctuations which occur in the output. To support this hypothesis, the following explanation is given.

Recall that there are fewer rays intersecting (and thus fewer tangent points occurring) at the inner radii than at the outer ones. Indeed, only one ray intersects the central radius. This means that the angular resolution in the center regions is considerably less than in the outer limits. Thus, any errors in angular variables will be more prominent in the center regions. It is thought that the errors are in the angular weights approximations. This theory was examined by varying the expansion of the intensity function and generating new angular weights for each expansion. The function was expanded in numerous ways including Chebyshev polynomials (Type I and II), variations of expansions in terms of the angle ϕ and the sine of the angle ϕ, and numerous expansions in terms of cosines of the angle ϕ. All of these expansions

effected the fluctuations in flux by some amount: all increasing the fluctuations. Only the Chebyshev polynomials, Type I, were close to the degree of fluctuation caused by the Lengendre expansion, but there was still no improvement. It is believed that there is still an as yet undiscovered variation of intensity expansion which will result in an even better fit of the program output to predicted results.

Now consider some of the other output produced as shown in Figures 12 - 14. In Figure 12, the opacity is shown as a reminder to the programmer of the opacity input. This figure also shows the source function and average intensity output at each radius. The moments ratios (Figure 13) show again how reasonably the ray-integration model obeys physical law. Recall that for the radiative equilibrium condition J=S in the atomosphere region, thus the ratio J/S should go quickly to one. Recall also that the Eddington approximation states that the Eddington factor f_k should be approximately 1/3 at the center, (isotropic limit), and progress toward 1. In addition, the ratio f_H is expected to go from 0 to 1 over the region of the sphere. The results shown in Figure 13 show good approximation of these conditions. The quantity J/S goes quickly to one and drops slightly at the end. This drop at the end can be explained by recalling that an extrapolated boundary was imposed on the sphere which numerically created an artifically high source function at the outer boundary, thus resulting in an artificially low J/S ratio, which the Unsold iteration was unable to correct for completely. Experimentation with other

boundary conditions are in order to rectify this condition.

As shown in Figure 13, the ratios f_k and f_H begin at the proper limits in the center of the sphere, (1/3 and 0 respectively) and build slowly toward one. The values do not quite reach one at the physical limit of the sphere because only beyond this limit does true streaming occur and the values of $f_k \rightarrow 1$ and $f_H \rightarrow 1$ actually occur.

Lastly, consider the solution to the moments equations shown in Figure 14. The solid line is the value of the Eddington flux solved for directly in the ray-integration technique and the other lines were formed by substituting in the other moments calculated to the moments equation and solving through for H. Note that, in the outer regions, all three equations agree very well. In the center regions of the sphere the solution of the zero'th moment seems high and the solution to the first moment seems low. These variations are also believed due to the inaccuracy of angular weights in the center regions of the sphere.

Case II

The first variation done, to experiment with the versatility of the program, was to introduce a deliberate perturbation to the input source function. This was done to see if the program would still iterate to the answer given in the first case, providing the mesh, power and opacity remained the same. The perturbation was to introduce an artificially high central source value by multiplying the source created by various values. The total flux radiation output by increasing the source

region by a factor of 2 appears in Figure 15. The flux, which the program iterated to, is exactly that of the first case. Several perturbations were introduced, all of which iterated to the same answer. This result indicates that the iteration technique used, in all cases, brought about equilibrium as near as it could, considering the lack of angular resolution.

Case III

Another variation done for verification was to alter the radius mesh of Case I, leaving all other parameters the same. The new radius mesh used also consisted of 23 radii, but a logarithmic spacing was used in which the spacing between radii increased moving out from the center to the physical boundry of the sphere. The output produced for the logarithmic mesh appear in Figures 16 through 19. Note that the results produced with the self-similar mesh are virtually the same as for the even mesh case. Fluctuations still occur within the inner regions of the sphere but, while not as large in magnitude, there are noticeably more of them.

This follows for the error existing in the angular weight calculated. That is, with smaller gaps between radii in the center of the sphere, the ds intervals integrated over will be smaller and more will exist closer to the center of the sphere. If the expansion used for the intensity (remember, this generates the production of angular weights) is not accurate, then the departures of the intensity from the true value might be more noticable over small segments sampled. With the logarithmic mesh used, there are more samplings of

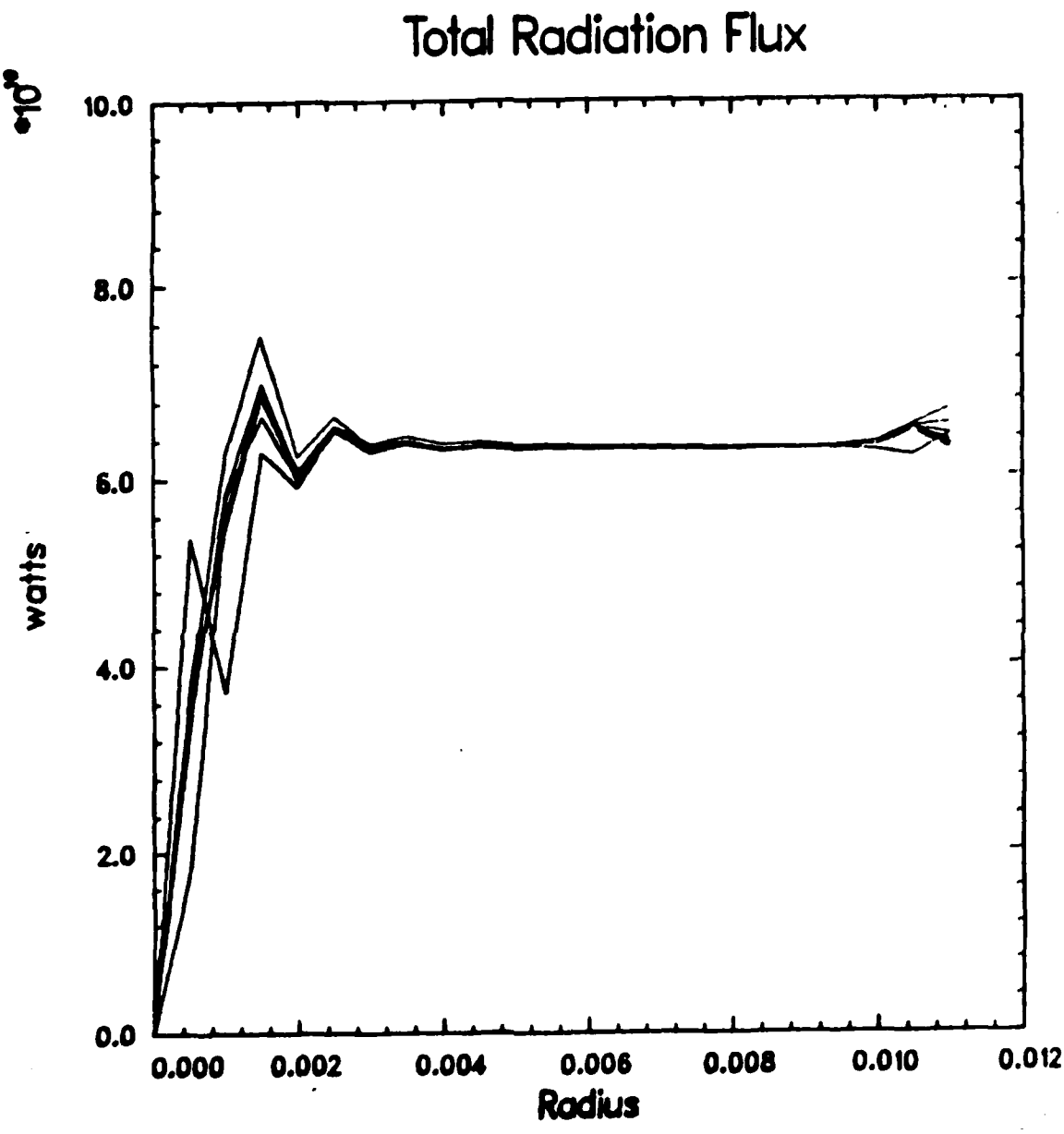

Figure 15

Total Radiation Flux (Case II)

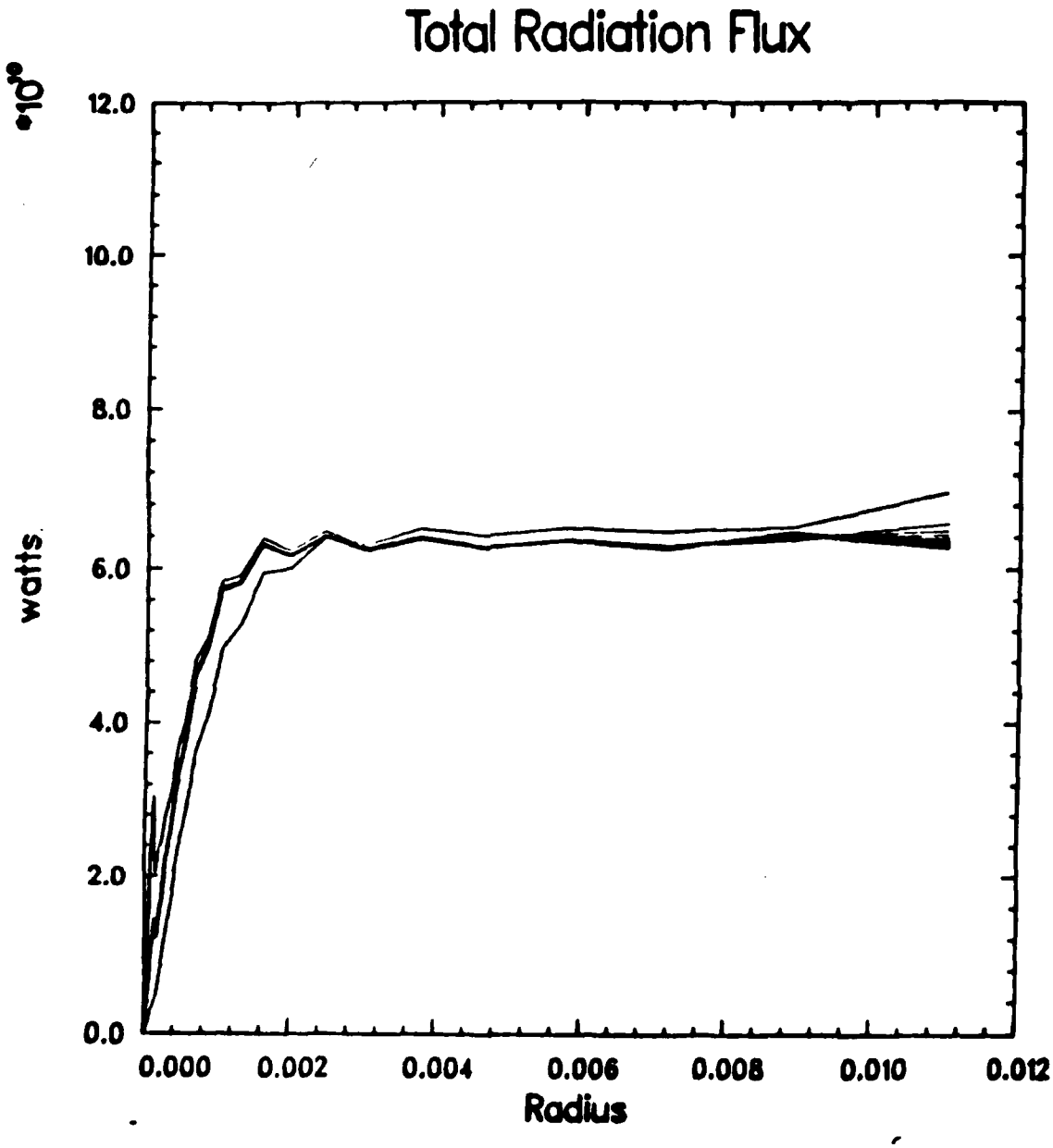

Figure 16

Total Radiation Flux (Case III)

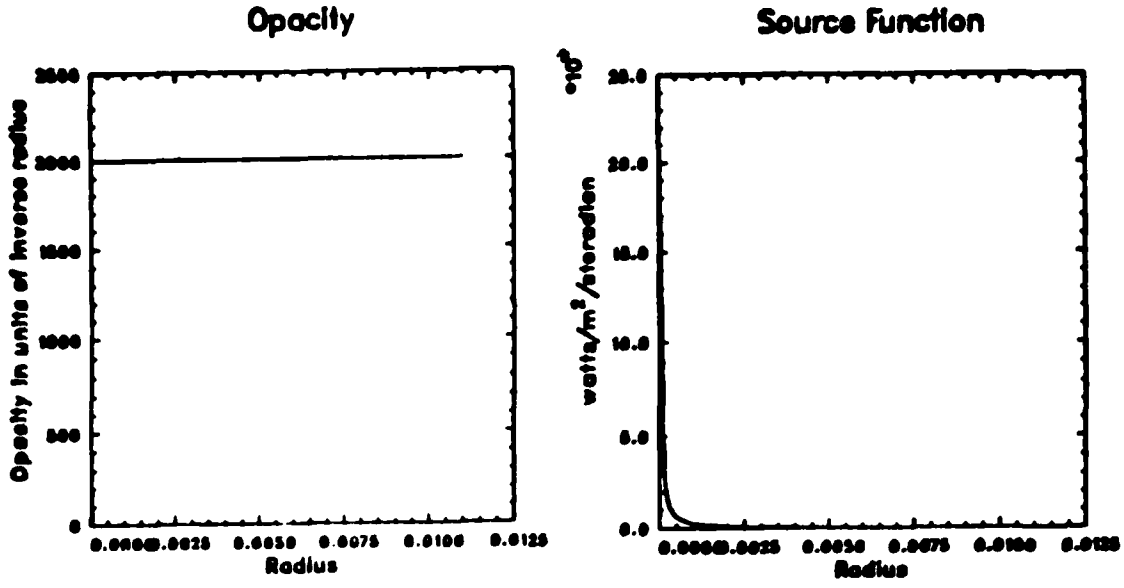

Figure 17

Opacity and Source Function (Case III)

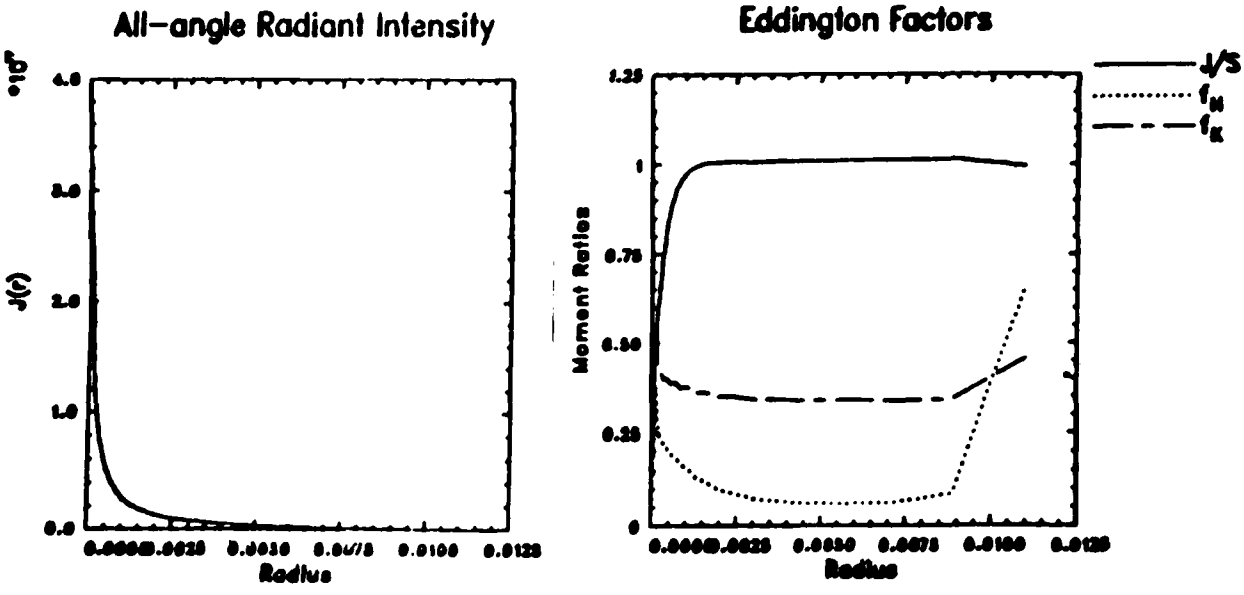

Figure 18

All-Angle Radiant Intensity and Eddington Factors (Case III)

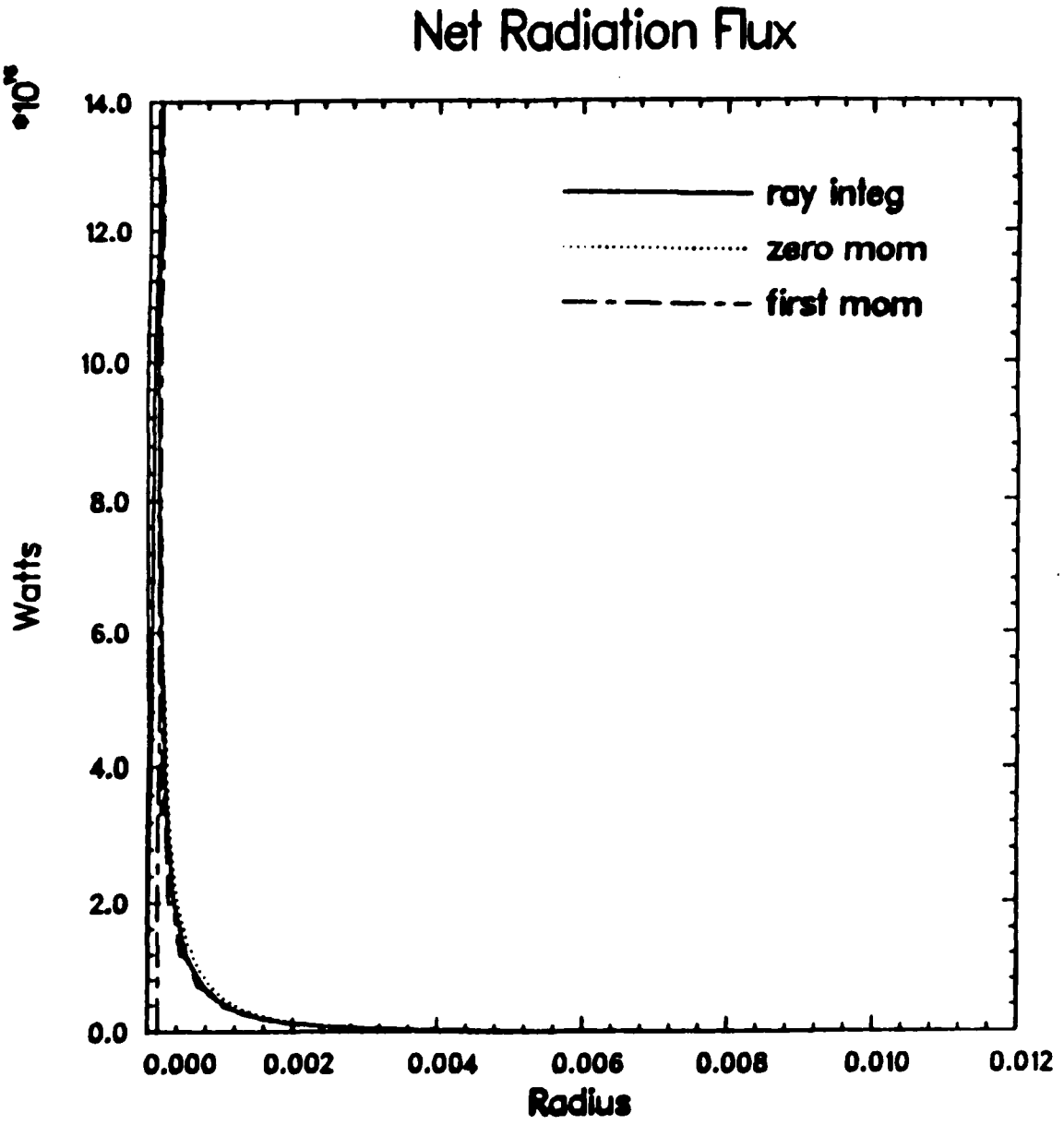

Figure 19

Net Radiation Flux (Case III)

the intensity taken at the inner radii of the sphere, thus more fluctuations will appear.

Consider the remainder of the output for this case, Figures 17 - 19). First, note that Figure 18 shows an improved agreement of J/S and f_k. There is still, however, fluctuation in f_H. Careful examination of the figure shows that f_H does start at zero, but rises quickly to approximately 1/4, but then drops and resumes its climb toward one. The sudden rise in f_H in the inner regions of the sphere occurs here for the same reason that it did in Case I, lack of angular resolution in the center.

Also note that the net radiation flux as illustrated in Figure 19 shows good agreement between the different techniques used to compute it.

VII. Conclusions and Recommendations

The preceding chapter has presented a series of cases for which the ray-integration technique was implemented. In these cases, reasonable agreement is made between the results produced and those expected from the physics of the situation. Inaccuracies still exist in three areas. Most obviously, the angular weights generated are not optimum. In addition, the boundary conditions used to generate the source function at the outer boundary is not optimum in that it produces an artificially high value at this limit.

It is suggested that further efforts be made to find the appropriate weight scheme and boundary condition for this program.

It is further recommended that the technique developed be expanded to applicability in a frequency dependent (i.e., non-grey atmosphere) problem. Also expansion should be made to make the technique valid for time varying energy flow.

Appendix A

Gaussian Quadrature

Given a definite integral

$$\int_a^b f(x)\, w(x)\, dx$$

where f(x) is some polynomial exisitng over the interval (a,b). This integral can be approximated by the sum

$$\sum_{k=1}^{n} f(X_k)\, A_k$$

which contains 2n + 1 parameters:

n x_k 's, points for evaluating f(x)

n A_k 's, coefficients

and

the choice of n itself

It was pointed out by Gauss that for unevenly spaced x points for an n'th degree polynomial, whichis orthogonal to all lower degree polynomials, that the A_k coefficients simply represented a set of weights. And that if these weights were multiplied by the function f(x) at the x interval, then the summation approximation to the integral would be exact. Some of the polynomials which fit these criterion are Legendre, Laguerre, Hermite, and Chebyshev (1:970-973).

Appendix B

Cubic Spline Interpolation

One method of obtaining an estimate values for a function which can be approximated as a polynomial over a large interval, is to the divide interval into a series of subintervals and construct a polynomial along each subinterval which generally follows the overall function in a pieceways manner. If the polynomial function being interpolated is of third order, then the method used is called cubic spline interpolation, and is described as follows.

Given a function f(x) defined on the interval a to b where the interval is divided into subintervals x such that $a < x_o < x_1 < \ldots < x_n < b$, a cubic spline interpolant, S, can be formed if the function, f, obeys the following conditions:

a) S is a cubic spline polynomial, denoted S_j, on the subinterval (x_j, x_{j+1}), for each j = 0, 1, ..., n - 1;

b) $S(x_j) = f(x_j)$, for each j = 0, 1, ..., n;

c) $S_j(x_{j+1}) = S_{j+1}(x_{j-1})$, for each j = 0, 1, ..., n - 2

d) $S'_j(x_{j+1}) = S'_{j+1}(x_{j+1})$ for each j = 0, 1, ..., n - 2

e) $S''_j(x_{j+1}) = S''_{j+1}(x_{j+1})$ for each j = 0, 1, ..., n - 2

f) one of the following set of boundary conditions is satisfied

(i) $S''(x_o) = S''(x_n) = 0$

(ii) $S''(x_o) = f''(x_o)$ and $S'(x_n) = f'(x_n)$

Using condition one the interpolant, S, is of the form

$$S_j(x) = a_j + b_j h + c_j h^2 + d_j h^3$$

where $h = (x - x_j)$, if:

$$a = f(b)$$

$$b = f'(b)$$

$$c = \frac{3(a - b)}{h} - \frac{(f'(a) + f'(b))}{h}$$

and

$$d = \frac{2(b - a)}{h} + \frac{(f'(a) + f'(b))}{h}$$

(5:116-128)

Appendix C

Glossary of Computer Terms

Term	Definition
a1/a2/a3	fits for opacity polynomial
bfac/cfac	fits for cubic spline interpolant
cosph1	cosine of angle at beginning of ds interval
cosph2	cosine of angle at end of ds interval
c(jj)	cosine of jj angle
delsor	S-J
etaui	$e^{-\tau}$
g(j)	opacity at j
gs(j)	slope of opacity at j
j	radius index
jn	number of radii
jw	tangent point index
j1/j2	# of radius at the beginning/end of the ds interval
hmom0	solution for H from zero moment equation
hmom1	solution for H from first moment equation
nfreq	number of iterations to be performed
phi(jj)	angle at tangent point jj
pprime	power/2*pi
psm1/pbig	estimates for gamma functions
p1 - 4	exact solution of tau integrals
sourc(j)	source function at j
radi	radiant intensity

radj(j)	all-angle radiant intensity at j
radh(j)	Eddington flux at j
radk(j)	second moment of intensity at j
rstar	r* function
rs1	dr(j1)/ds
rs1	dr(j2)/ds
r0	impact parameter
r1/r2	values of the radii at the beginning/end of the ds interval
sstar	S* function
tau0	opacity along line of sight
t1 - 4	solution to tau integral
w(jw)	weight at interval jw

APPENDIX D

SOURCE CODE

```
$OPTIONS S=600,D=10,A=40,X
C       ------------------------------------
C       BEGIN PROGRAM BY INITIALIZING ARRAYS
C       ------------------------------------
        DIMENSION R(25),WGHT(700),TAUE(10)
        DIMENSION G(25),GS(25),TAUO(325),SOURC(25),C(325
        DIMENSION P1(325),P2(325),P3(325),P4(325)
        DIMENSION RADJ(25),RADH(25),RADK(25),FLUX(25)
        DIMENSION DELSOR(25),HMOMO(25),HMOM1(25)
        REAL MSQR
        TYPE'THE PROGRAM HAS BEGUN'
C       ---------------
C       READ INPUT FILE
C       ---------------
        CALL OPEN (5,'LFILE.TXT",IERROR)
        IF (IERROR .NE. 0) THEN
                           TYPE 'CANNOT OPEN INPUT FILE'
                           STOP 'RUN ABORTED'
                           ENDIF
        READ (5,*) JN,(R(I),I=1,JN),A1,A2,A3,A4,A5,A6
C       ----------------------------------------
C       PRINT INPUT FILE AND INITIALIZE CONSTANTS
C       ----------------------------------------
        TYPE'JN= ',JN
        TYPE'RADII= '
        WRITE (1,1) (R(I),I=1,JN)
1       FORMAT(F7.4)
        TYPE 'A1= ',A1
        TYPE 'A2= ',A2
        TYPE 'A3= ',A3
        TYPE 'POWER= ',A4
        TYPE 'NFREQ= ',A5
        TYPE 'START= ',A6
        START=A6
        POWER=A4
        NFREQ=A5
        ITER=0
        PI=3.141592654
        PPRIME=ABS(POWER/(2*PI))
C       ------------------------------------------------
C       CALL SUBROUTINE TO CALCULATE ANGULAR VARIABLES
C       ------------------------------------------------
        TYPE 'BEGIN GENERATION OF PHI DEPENDENT VARIABLES'
        CALL XFAC (JN,R,WGHT,C,P1,P2,P3,P4)
        TYPE 'END GENERATION OF PHI DEPENDENT VARIABLES'
C       ------------------------------------
C       CALCULATE OPACITY AND SLOPE OF OPACITY
C       ------------------------------------
```

```
49:           JNM=JN-1
50:           JNM2=JNM-1
51:           DO 100 J=1,JN
52:           G(J)=(A3*R(J)+A2)*R(J)+A1
53:   100     GS(J)=2.0*A3*R(J)+A2
54:   C       ---------------------------------------
55:   C       CALCULATE 'FIRST GUESS'SOURCE FUNCTION
56:   C       ---------------------------------------
57:           SOURC(JN)=PPRIME/(R(JN)*R(JN))
58:           DO101 JP=1,JNM2
59:           J=JN-JP
60:           SOURC(J)=SOURC(J+1)+(R(J+1)-R(J))*0.75*PPRIME
61:        1  *(G(J+1)/(R(J+1)*R(J+1))+G(J)/(R(J)*R(J)))
62:   101     CONTINUE
63:           SOURC(1)=SOURC(2)+START*PPRIME*G(2)/R(2)
64:   C       ---------------------------------------
65:   C       ---------------------------------------
66:   C       BEGIN MAJOR LOOP TO CALCULATE ALL RAYS
67:   C       ---------------------------------------
68:   C       ---------------------------------------
69:           DO 3000 NT=1,NFREQ
70:   C       -----------------------------------
71:   C       CALCULATE TAU FOR EACH DS SEGMENT
72:   C       -----------------------------------
73:           DO 300 JZP=1,JNM
74:           JZ=JN-JZP
75:           DO 280 JK=1,JZP
76:           JI=JZP*(JZP-1)/2+JK
77:           J1=JN-JZP+JK-1
78:           J2=J1+1
79:           R1=R(J1)
80:           R2=R(J2)
81:           DR=R2-R1
82:           DR2=DR*DR
83:           DR3=DR2*DR
84:           BB=(3.*G(J2)-3.*G(J1)/DR2-(GS(J2)+2.*GS(J1))/DR
85:           CC=(GS(J2)+GS(J1))/DR2-2.*(G(J2)-G(J1))/DR3
86:           T1=(((-CC)*R1+BB)*R1-GS(J1))*R1+G(J1)
87:           T2=((3.*CC)*R1-2.*BB)*R1+GS(J1)
88:           T3=-3.*CC*R1+BB
89:           T4=CC
90:   280     TAUO(JI)=T1*P1(JI)+T2*P2(JI)+T3*P3(JI)+T4*P4(JI)
91:   300     CONTINUE
92:   C       ---------------------------------------
93:   C       INITIALIZE ALL INTENSITY MOMENTS TO ZERO
94:   C       ---------------------------------------
95:           DO 350 J=1,JN
96:           RADJ(J)=0.0
97:           RADH(J)=0.0
98:   350     RADK(J)=0.0
99:           JJ=0
```

```
100:  C     ---------------------------------
101:  C     BEGIN CALCULATIONS FOR ENTIRE RAY
102:  C     ---------------------------------
103:        DO 400 JZP=1,JNM
104:        JZ=JN-JZP
105:        RO=R(JZ)
106:        COSPH2=C(JN*(JN-1)/2+JZ
107:        IF (NT .EQ. 100) WRITE(1,1111)JZ
108:  1111  FORMAT('  JZ='I2/,'J1  J2  JJ',3X,'R1',6X,'R2',
109:       1     7X,'G1',10X,'G2',6X,'TAU',8X,'C1',4X,'C2',
110:       2    7X,'S1',9X,'S2',9X,'SSTAR')
111:        J1=JN+1
112:        RADI=0.0
113:  C     ----------------------------
114:  C     CALCULATE 'INWARD-GOING' RAY
115:  C     ----------------------------
116:        DO 380 JK=1,JZP
117:        JJ=JJ+1
118:        J1=J1-1
119:        J2=J1-1
120:        R1=R(J1)
121:        R2=R(J2)
122:        G1=G(J1)
123:        G2=G(J2)
124:        JW=J2*(J2-1)/2+JZ
125:        JI=JZP*(JZP-1)/2+J1-JZ
126:        COSPH1=COSPH2
127:        COSPH2=C(JW)
128:        TAU=TAUO(JI)
129:        RS1=COSPH1/G1
130:        RS2=COSPH2/G2
131:        BFAC=(3.*(R1-R2)/TAU-(RS1+2.*RS2))/TAU
132:        CFAC=(-2.*(R1-R2)/TAU+RS1+RS2)/TAU/TAU
133:        ETAUI=EXP(-TAU)
134:        PSML=((0.08333333*TAU-0.2)*TAU+0.25)*TAU**4
135:        PBIG=6.-(((1.02228*TAU+3.00939)*TAU+5.02488)
136:       1   *TAU+5.1244)*ETAUI
137:        TI3=PSML*PBIG/(PSML+PBIG)
138:        TERM=TAU*TAU*TAU*TAU*ETAUI
139:        TI2=0.333333*(TI3+TERM)
140:        TERM=TERM/TAU
141:        TI1=0.5*(TI2+TERM)
142:        TERM=TERM/TAU
143:        TIO=TI1+TERM
144:        RSTAR=R2+(RS2*TI1+BFAC*TI2+CFAC*TI3)/TIO
145:        C1=(R2-RSTAR)/(R2-R1)
146:        C2=(RSTAR-R1)/(R2-R1)
147:        SSTAR=C1*SOURC(J1)+C2*SOURC(J2)
148:  C     *********************************
149:  C           TRANSFER EQUATION
150:  C     *********************************
151:        RADI=RADI*ETAUI+SSTAR*(1.-ETAUI)
152:  C     *********************************
```

```
      If (NT .EQ, 100) WRITE(1,1112) J1,J2,JJ,R1,R2,G1,
     1  G2,TAU,C1,C2,SOURC(J1),SOURC(J2),SSTAR
1112  FORMAT(2I3,I4,2F7.4,2E11.2,E11.3,2F7.3,3E12.4)
C     ------------------
C     ACUMMULATE MOMENTS
C     ------------------
      DRAD=RADI*WGHT(JW)
      WPERP=-C(JW)
      RADJ(J2)=RADJ(J2)+DRAD
      DRAD=DRAD*WPERP
      RADH(J2)=RADH(J2)+DRAD
!c$:  DRAD=DRAD+WPERP
      RADK(J2)=RADK(J2)+DRAD
380   CONTINUE
      JZ1=JZP+1
      JZ2=2*JZP
      J1=JZ-1
C     ----------------------------
C     CALCULATE 'OUTWARD-GOING' RAY
C     ----------------------------
      DO 390 JK=JZ1,JZ2
      JJ=JJ+1
      J1=J1+1
      J2=J1+1
      R1=R(J1)
      R2=R(J2)
      G1=G(J1)
      G2=G(J2)
      JW=J2*(J2-1)/2+JZ
      JI=JZP*(JZP-1)/2+J2-JZ
      COSPH1=COSPH2
      COSHP2=C(JW)
      TAU=TAU0(JI)
      RS1=-COSPH1/G1
      RS2=-COSPH2/G2
      BFAC=(3.*(R1-R2)/TAU-(RS1+2.*RS2))/TAU
      CFAC=(-2.*(R1-R2)/TAU+RS1+RS2)/TAU/TAU
      ETAUI=EXP(-TAU)
      PSML=((0.08333333*TAU-0.2)*TAU+0.25)*TAU**4
      PBIG=6.-(((1.02228*TAU+3.00939)*TAU+5.02488)
     1   *TAU+5.1244)*ETAUI
      TI3=PSML*PBIG/(PSML+PBIG)
      TERM=TAU*TAU*TAU*ETAUI
      TI2+0.333333*(TI3+TERM)
      TERM=TERM/TAU
      TI1=0.5*(TI2+TERM)
      TERM=TERM/TAU
      TI0=TI1+TERM
      RSTAR=R2+(RS2*TI1+BFAC*TI2+CFAC*TI3)/TI0
      C1=(R2-RSTAR)/(R2-R1)
      C2=(RSTAR-R1)/(R2-R1)
      SSTAR=C1*SOURC(J1)+C2*SOURC(J2)
```

```
C     *********************************
C            TRANSFER EQUATION
C     *********************************
      RADI=RADI*ETAUI+SSTAR*(1.-ETAUI)
C     *********************************
      IF (NT .EQ. 100) WRITE (1,1112) J1,J2,JJ,R1,R2,
     1  G1,G2,TAU,C1,C2,SOURC(J1),SOURC(J2),SSTAR
C     ------------------
C     ACUMMULATE MOMENTS
C     ------------------
      DRAD=RADI*WGHT(JW)
      WPERP=C(JW)
      RADJ(J2)=RADJ(J2)+DRAD
      DRAD=DRAD*WPERP
      RADH(J2)=RADH(J2)+DRAD
      DRAD=DRAD*WPERP
      RADK(J2)=RADK(J2)+DRAD
 390  CONTINUE
C     -------------------------------
C     GO BACK AND CALCULATE NEXT RAY
C     -------------------------------
      RADH(1)=0.0
      RADK(1)=RADK(1)/3.0
 400  CONTINUE
      DELSOR(1)=SOURC(1)-RADJ(1)
      DO 440  J=2,JN
      DELSOR(J)=SOURC(J)-RADJ(J)
C     ----------------------------------
C     DEFINE AND PRINT FLUX FOR ALL RADII
C     ----------------------------------
      FLUX(J)=4*PI*(R(J)*R(J))*RADH(J)
 440  CONTINUE
      RADH(1)=0.0
      FLUX(1)=0.0
      IF (NT .EQ. 100) GO TO 441
      ITER=ITER+1
      TYPE
      TYPE 'ITERATION ',ITER
      TYPE 'TOTAL RADIATION FLUX    RADIUS'
      DO 557 I=1,JN
      WRITE (1,557) FLUX(I),R(I)
 557  FORMAT (E11.3,30X,F7.4)
 441  CONTINUE
      IF (POWER .GT. 0.0) GO TO 445
C     ---------------------------------
C     DO LAMBDA ITERATION FOR THIN CASES
C     ---------------------------------
      SOURC(1)=0.0
      DO 443 J=2,JN
 443  SOURC(J)=RADJ(J)
      GO TO 449
 445  CONTINUE
```

```
C     ------------------------------------
C     DO UNSOLD ITERATION FOR THICK CASES
C     ------------------------------------
      SOURC(JN)=SOURC(JN)*PPRIME/(2.*R(JN)*R(JN)
     1    /RADH(JN)
      DO 446 JP=1,JNM2
      J=JN-JP
      CON=(R(J+1)-R(J))*0.5
      A=CON*G(J)*RADJ(J)/RADK(J)
      B=CON*G(J+1)*RADJ(J+1)/RADK(J+1)
      SOURC(J)=(RADJ(J)-A*RADH(J))*(SOURC(J+1)+B*PPRIME/(2.*
     1    R(J+1)*R(J+1)))/(RADJ(J+1)+B*RADH(J+1))+A*PPRIME/
     2    (2.*R(J)*R(J))
446   CONTINUE
      B=A
      CON=R(2)*0.5
      A=CON*G(1)*RADJ(1)/RADK(1)
      SOURC(1)=(RADJ(1)-A*RADH(1))*(SOURC(2)+B*PPRIME/(2.*
     1   R(2)*R(2)))/(RADJ(2)+B*RADH(2))
      SOURC(1)=SOURC(1)+(PPRIME/(2.*R(2)*R(2)*RADH(2)))*
     1    (SOURC(1)-RADJ(1))
449   CONTINUE
3000  CONTINUE
C     ----------------------------------------
C     SOLVE FIRST AND ZERO'TH MOMENT EQUATIONS
C     ----------------------------------------
      HMOM0(1)=0.0
      HMOM1(1)=0.0
      DO 455 J=2,JNM
      RBAR=0.5*(R(J-1)*R(J-1)+R(J)*R(J))
      RDIFF=R(J)-R(J-1)
      RHSBAR=0.5*(G(J-1)*DELSOR(J-1)+G(J)*DELSOR(J))
      HMOM0(J)=R(J-1)*R(J-1)*HMOM0(J-1)/(R(J)*R(J))
     1   +RDIFF*RBAR*RHSBAR/(R(J)*R(J))
455   HMOM1(J)=-((RADK(J+1)-RADL(J-1))/(R(J+1)-R(J-1))
     1   +(3.0*RADK(J)-RADJ(J))/R(J))/G(J)
      HMOM1(JN)=-((RADK(JN)-RADK(JN-1))/(R(JN)-R(JN-1))
     1   +(3.0*RADK(JN)-RADJ(JN))/R(JN))/G(JN)
C     ------------
C     PRINT OUTPUT
C     ------------
      TYPE
      TYPE
      TYPE 'OPACITY                RADIUS'
      DO 149 I=1,JN
      WRITE (1,150) G(I),R(I)
150   FORMAT (E11.3,7X,E11.3)
149   CONTINUE
      TYPE
      TYPE
      TYPE 'SOURCE                 RADIUS'
      TYPE'FUNCTION'
      DO 151 I=1,JN
```

```
310:       WRITE (1,150) SOURC(I),R(I)
311: 151   CONTINUE
312:       TYPE
313:       TYPE
314:       TYPE 'ALL ANGLE              RADIUS'
315:       TYPE 'RADIANT INTENSITY'
316:       DO 152 I=1,JN
317:       WRITE (1,150) RADJ(I),R(I)
318: 152   CONTINUE
319:       TYPE
320:       TYPE
321:       TYPE '*************EDDINGTON FACTOR*****************'
322:       TYPE
323:
324:       TYPE' J/S      H/J       K/J     RADIUS'
325:       DO 500 J=1,JN
326:       RADH(J)=RADH(J)/RADJ(J)
327:       RADK(J)=RADK(J)/RADJ(J)
328:       TFAC=0.0
329:       IF (SOURC(J) .NE. 0.0) TFAC=1./SOURC(J)
330:       RADJ(J)=TFAC*RADJ(J)
331:       WRITE (1,499) RADJ(J),RADH(J),RADK(J),R(J)
332: 499   FORMAT (3(E11.3,4X),F7.4)
333: 500   CONTINUE
334: C
335: C
336:       TYPE
337:       TYPE
338:       TYPE'********* NET RADIATION FLUX ************'
339:       TYPE
340:       TYPE'RAY INTEG   ZERO MOM   FIRST MOM   RADIUS'
341:       DO 505 J=1,JN
342:       RADH(J)=RADH(J)*SOURC(J)
343:       WRITE (1,251) RADH(J),HMOMO(J),HMOM1(J),R(J)
344: 251   FORMAT (3(E11.3,4X),F7.4)
345: 505   CONTINUE
346:       END
347: C     --------------------------------
348: C     BEGIN GEOMETRY FACTOR SUBROUTINE
349: C     --------------------------------
350: $OPTIONS S=200,X
351:       SUBROUTINE XFAC(JN,R,WGHT,C,P1,P2,P3,P4)
352:       DIMENSION PHI(325),W(325),R(25),WGHT(700),C(700)
253:       DIMENSION P1(250),P2(250),P3(250),P4(250)
354:       REAL MSQR
355:       PI-3.14159265
356: C     ----------------------------------------
357: C     CALCULATE PHI ANGLES AND ANGULAR WEIGHTS
358: C     ----------------------------------------
359:       C(1)=1.0
360:       C(2)-1.0
361:       C(3)=0.0
362:       C(4)=1.0
```

```
      C(5)=SQRT(1.-((R(2)*R(2))/(R(3)*R(3))))
      C(6)=0.0
      WGHT(1)=1.0
      WGHT(2)=1./6.
      WGHT(3)=2./3.
      WGHT(4)=-0.099955
      WGHT(5)=0.3556495677
      WGHT(6)=0.4889186828
      JJ=7
      JNM=JN-1
      DO 1000 KK=4,JN
      KMAX=2*KK-1
      DO 4 K=1,KMAX
4     W(K)=0.0
      KKP=KK+1
      DO 10 K=1,KK
      TESTX=R(K)/R(KK)
      TESTY=SQRT(1.-TESTX*TESTX)
      IF (TESTY .NE. 0.0) GO TO 23
      PHI(K)=90.0*.0174532925
      GO TO 24
23    ARG=TESTX/TESTY
      PHI(K)=ATAN(ARG)
24    CONTINUE
10    CONTINUE
      DO 20 K=KKP,KMAX
20    PHI(K)=PI-PHI(KMAX-K+1)
      DO 100 K=2,KMAX,2
      FM=PHI(K-1)
      FO=PHI(K)
      FP=PHI(K+1)
      CP=COS(FP)
      CO=COS(FO)
      CM=COS(FM)
      DF=CM-CP
      DS=(CM*CM-CP*CP)/2.
      DS2=(CM*CM*CM-CP*CP*CP-CM+CP)/2.
      PSQR=(3.*CP*C:-1.)/2.
      OSQR=(3.*CO*CO-1.)/2.
      MSQR=(3.*CM*CM-1.)/2.
      DEN=(CO*PSQR-CP*OSQR)+(CP*MSQR-CM*PSQR)
     1    +(CM*OSQR-CO*MSQR)
      DWN=(CO*PSQR-CP*OSQR)*DF+(OSQR-PSQR)*DS+(CP-CO)*DS2
      DWO=(CP*MSQR-CM*PSQR)*DF+(PSQR-MSQR)*DS+(CM-CP)*DS2
      DWP=(CM*OSQR-CO*MSQR)*DF+(MSQR-OSQR)*DS+(CO-CM)*DS2
      W(K-1)=W(K-1)+DWM/DEN
      W(K)=DWO/DEN
      W(K+1)=W(K+1)+DWP/DEN
100   CONTINUE
      DO 110 K=1,KK
      C(JJ)=COS(PHI(K))
      WGHT(JJ)=W(K)/2.
110   JJ=JJ+1
```

```
 1000 CONTINUE
      TYPE'FINISH GENERATION OF COSINES AND WEIGHTS'
C     ----------------------------------
C     BEGIN GENERATION OF P1-P4 CONSTANTS
C     ----------------------------------
      TYPE'BEGIN GENERATION OF P1-P4 CONSTANTS'
      DO 2000 JZP=1,JNM
      JZ=JN-JZP
      JK1=JZP*(JZP-1)/2+1
      JK2=JK1+JZP-1
      DLAST=0.0
      ELAST=0.0
      IF (JZ .NE. 1) ELAST=ALOG(R(JZ))
      DO 2000 JK=JK1,JK2
      J1=JZ+JK-JK1
      J2=J1+1
      R1=R(J1)
      R2=R(J2)
      RO=R(JZ)
      DNOW=SQRT(R2*R2-RO*RO)
      DD=R2+DNOW
      ENOW=0.0
      IF (DD .GT. 0.0) ENOW=ALOG(DD)
      P1(JK)=DNOW-DLAST
      P2(JK)=(R2*DNOW-R1*DLAST+RO*RO*RO*(ENOW-ELAST))*0.5
      P3(JK)=((R2*R2+2.0*RO*RO)*DNOW-(R1*R1+2.0*RO*RO)
     1   *DLAST(*0.33333
      P4(JK)=0.25*R2*DNOW*(R2*R2+1.5*RO*RO)+0.375
     1   *RO*RO*RO*RO*ENOW-0.25*R1*DLAST
     2  *(R1*R1+1.5*RO*RO)-0.375*RO*RO*RO*ELAST
      DLAST=DNOW
      ELAST=ENOW
 2000 CONTINUE
      RETURN
      END
```

Bibliography

1. Arfken, George, ed. Mathematical Methods for Physicists (Third Edition). Ordando: Academic Press, Inc., 1985.

2. Aier, L. H. Difference Equations and Linearizatgion Methods for Radiative Transfer. Los Alamos National Laboratory Publication. Los Alamos National Laboratory, Los Alamos, New Mexico.

3. Bowers, Richard L. and Deeming, Terry. "Radiation and Energy Transport," Astrophysics I, Stars. Boston: Jones and Bartlett Publishers, Inc., 1984.

4. Bridgman, Charles J. The Physics of Nuclear Explosives, Chapter 2 and Chapter 3. Class Notes. School of Engineering, Air Force Institute of Technology (AU), Wright Patterson AFB, Ohio.

5. Burden, Richard L. et al. Numerical Analysis. Boston: Prindle, Weber and Schmidt, 1978.

6. Chandrasekhar, S. Radiative Transfer. London: Oxford University Press, 1950.

7. Mihalas, Dimitri. Stellar Atmospheres. San Francisco: W. H. Freeman and Company, 1978.

8. Nickel, George. Lecture Materials Provided in Personal Interview, 10-14 June, 1985.

9. Unsold, A. Physik der Sternatmosharen. Berlin: Springer-Verlag, 1955.

Vita

Susan Elizabeth Durham was born October 26, 1958 in Norwich, Connecticut. She graduated from the Norwich Free Academy High School and enlisted in the U. S. Air Force in 1976. She worked as a crew chief and Aircraft Maintenance Mechanic at Shaw A. F. B. in South Carolina for two years before being granted entry to the Air Force's Airmen Scholarship and Commissioning Program, (ASCP). In accordance with terms of the ASCP, she was discharged and attended college under the auspices of the government. In 1982, she graduated from Georgia State University and was commissioned into the Air Force. She worked as an Orbital Analyst and Analyst trainer at Eglin A. F. B. in Florida before being admitted to the Air Force Institute of Technology in 1984.

AD-A172 770 THE RAY-INTEGRATION TECHNIQUE IN SPHERICAL GEOMETRY(U) 2/2
AIR FORCE INST OF TECH WRIGHT-PATTERSON AFB OH SCHOOL
OF ENGINEERING S E DURHAM MAR 86 AFIT/GNE/ENP/86M-3
UNCLASSIFIED F/G 20/9 NL

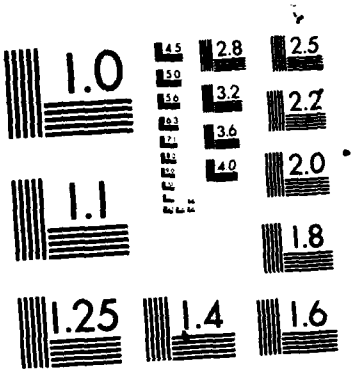

UNCLASSIFIED
SECURITY CLASSIFICATION OF THIS PAGE

AD-A172 770

REPORT DOCUMENTATION PAGE

1a. REPORT SECURITY CLASSIFICATION: UNCLASSIFIED	1b. RESTRICTIVE MARKINGS
2a. SECURITY CLASSIFICATION AUTHORITY	3. DISTRIBUTION/AVAILABILITY OF REPORT: Approved for public release; distribution unlimited
2b. DECLASSIFICATION/DOWNGRADING SCHEDULE	
4. PERFORMING ORGANIZATION REPORT NUMBER(S): AFIT GNE AFOT/~~CME~~/ENP/86M-3	5. MONITORING ORGANIZATION REPORT NUMBER(S)
6a. NAME OF PERFORMING ORGANIZATION: School of Engineering, Air Force Institute of Technology	6b. OFFICE SYMBOL (If applicable): AFIT/ENG
6c. ADDRESS (City, State and ZIP Code): Wright-Patterson AFB, Ohio 45433	7a. NAME OF MONITORING ORGANIZATION
8a. NAME OF FUNDING/SPONSORING ORGANIZATION: Los Alamos National Lab	8b. OFFICE SYMBOL (If applicable): X2
8c. ADDRESS (City, State and ZIP Code): Los Alamos, NM 87454	7b. ADDRESS (City, State and ZIP Code)
11. TITLE (Include Security Classification): See Box 19	9. PROCUREMENT INSTRUMENT IDENTIFICATION NUMBER
	10. SOURCE OF FUNDING NOS. — PROGRAM ELEMENT NO. / PROJECT NO. / TASK NO. / WORK UNIT NO.

Approved for public release: IAW AFR 190-1.
LYNN E. WOLAVER
Dean for Research and Professional Development
Air Force Institute of Technology (AU)
Wright-Patterson AFB OH 45433
9 May 86

12. PERSONAL AUTHOR(S): Susan E. Durham, B.S., 1Lt, USAF			
13a. TYPE OF REPORT: MS Thesis	13b. TIME COVERED: FROM _____ TO _____	14. DATE OF REPORT (Yr., Mo., Day): 1986 March	15. PAGE COUNT: 95

16. SUPPLEMENTARY NOTATION

17. COSATI CODES			18. SUBJECT TERMS (Continue on reverse if necessary and identify by block number)
FIELD	GROUP	SUB. GR.	Radiation Transport, Stellar Atmospheres, Grey Atmosphere, Equation of Radiative Transfer
20	09		

19. ABSTRACT (Continue on reverse if necessary and identify by block number)

Title: THE RAY-INTEGRATION TECHNIQUE IN SPHERICAL GEOMETRY

Thesis Chairmen: Charles J. Bridgman, George H. Nickel

A method of solution for the equation of radiative transfer for a spherical, grey atmosphere, steady state plasma in radiative eqiuilibrium is developed. The method is called the ray-integration technique and derives from the same method of solution done in cylinder geometry ~~by George Nickel of~~, Los Alamos National Laboratory. The total and net radiation flux, source function, opacity and moments of intensity are calculated as a function of radius. The solution to the zero'th

20. DISTRIBUTION/AVAILABILITY OF ABSTRACT: UNCLASSIFIED/UNLIMITED ☐ SAME AS RPT. ☐ DTIC USERS ☐	21. ABSTRACT SECURITY CLASSIFICATION: UNCLASSIFIED

22a. NAME OF RESPONSIBLE INDIVIDUAL: Charles J. Bridgman	22b TELEPHONE NUMBER (Include Area Code): (513) 255-4498	22c OFFICE SYMBOL: AFIT/ENP

DD FORM 1473, 83 APR — EDITION OF 1 JAN 73 IS OBSOLETE.

UNCLASSIFIED
SECURITY CLASSIFICATION OF THIS P

and first moment equations are also provided.

The conditions of the grey atmosphere problem and the general nature of radiation transport in spherical geometry are developed and the ray-integration technique, as applied to the problem, is presented.

Numerical results are calculated for a variety of radial mesh and opacities. These results are provided in graphic form and compared against theoretically predicted behavior.

The ray-integration technique developed in this thesis produces numerical results which are in reasonable agreement with theoretical predicted results.

END

11-86

DTIC